Published in final edited form as:
J Comp Neurol. 2013 August 1; 521(11): 2502–2522. doi:10.1002/cne.23295.

GABAergic Inputs from Direct and Indirect Striatal Projection Neurons Onto Cholinergic Interneurons in the Primate Putamen

Kalynda Kari Gonzales[1,3], **Jean-Francois Pare**[1,3], **Thomas Wichmann**[1,2,3], and **Yoland Smith**[1,2,3,*]

[1]Yerkes National Primate Research Center, Emory University, Atlanta, Georgia 30329

[2]Department of Neurology, Emory University, Atlanta, Georgia 30329

[3]Udall Center of Excellence for Parkinson's Disease Research, Emory University, Atlanta, Georgia 30329

Abstract

Striatal cholinergic interneurons (ChIs) are involved in reward-dependent learning and the regulation of attention. The activity of these neurons is modulated by intrinsic and extrinsic γ-aminobutyric acid (GABA)ergic and glutamatergic afferents, but the source and relative prevalence of these diverse regulatory inputs remain to be characterized. To address this issue, we performed a quantitative ultrastructural analysis of the GABAergic and glutamatergic innervation of ChIs in the postcommissural putamen of rhesus monkeys. Postembedding immunogold localization of GABA combined with peroxidase immunostaining for choline acetyltransferase showed that 60% of all synaptic inputs to ChIs originate from GABAergic terminals, whereas 21% are from putatively glutamatergic terminals that establish asymmetric synapses, and 19% from other (non-GABAergic) sources of symmetric synapses. Double pre-embedding immunoelectron microscopy using substance P and Met-/Leu-enkephalin antibodies to label GABAergic terminals from collaterals of “direct” and “indirect” striatal projection neurons, respectively, revealed that 47% of the indirect pathway terminals and 36% of the direct pathway terminals target ChIs. Together, substance P- and enkephalin-positive terminals represent 24% of all synapses onto ChIs in the monkey putamen. These findings show that ChIs receive prominent GABAergic inputs from multiple origins, including a significant contingent from axon collaterals of direct and indirect pathway projection neurons.

Indexing Terms

medium spiny neurons; substance P; enkephalin; GABA; striatum

The dorsal striatum receives glutamatergic inputs from all functional regions of the cerebral cortex and thalamus (Parent and Hazrati, 1995; Smith et al., 2004, 2009) and sends γ-

*CORRESPONDENCE TO: Yoland Smith, Yerkes National Primate Research Center, Emory University, 954 Gatewood Road NE, Atlanta, GA 30329. ysmit01@emory.edu.

Conflict of Interest Statement: None of the authors of this paper have a conflict of interest with other people or organizations.

Role of Authors: All authors had full access to all the data in the study and take responsibility for the integrity of the data and the accuracy of the data analysis. Study concept and design: K.K. Gonzales, Y. Smith, and T. Wichmann. Acquisition of data: K.K. Gonzales and J.-F. Pare. Analysis and interpretation of data: K.K. Gonzales, J.-F. Pare, and Y. Smith. Drafting of the manuscript: K.K. Gonzales, Y. Smith, and T. Wichmann. Critical revision of the manuscript for important intellectual content: K.K. Gonzales, Y. Smith, and T. Wichmann. Statistical analysis: K.K. Gonzales. Obtained funding: K.K. Gonzales, Y. Smith, and T. Wichmann. Administrative, technical, and material support: J.-F. Pare. Study supervision: K.K. Gonzales, J.-F. Pare, Y. Smith, and T. Wichmann.

aminobutyric acid (GABA)ergic projections to the external and internal segments of the globus pallidus (GPe and GPi) and the substantia nigra pars reticulata (SNr) via the so-called "direct and indirect" pathways (Albin et al., 1989; Alexander et al., 1990; Gerfen et al., 1990). The basal ganglia output nuclei (i.e., the GPi and SNr) relay this information back to the cerebral cortex and striatum via the thalamus (Alexander et al., 1990; Smith et al., 2004, 2009). Processing of information within the dorsal striatum involves dopaminergic inputs from the substantia nigra pars compacta (SNc), GABAergic afferents from the GPe, and intrastriatal GABAergic and cholinergic interneurons (Galvan and Wichmann, 2007; Wilson, 2007; Tepper et al., 2008; Gerfen and Surmeier, 2011).

In rodents, the striatum comprises 95% projection neurons (i.e., medium spiny neurons; MSNs) and 5% interneurons (Kemp and Powell, 1971; Wilson and Groves, 1980; Graveland and DiFiglia, 1985; Bolam et al., 2000), whereas in primates, interneurons account for as much as 24% of the striatal neuron population (Pasik et al., 1976; Graveland and DiFiglia, 1985; Roberts et al., 1996; Wu and Parent, 2000). The large cholinergic interneurons (ChIs) have long been recognized as important constituents of the striatal microcircuitry. ChIs give rise to extensive intrastriatal axonal arborizations and harbor thick primary dendrites with highly branched and varicose distal dendritic processes (Difiglia et al., 1980; Chang and Kitai, 1982; DiFiglia and Carey, 1986; Yelnik et al., 1991). ChIs are evenly distributed throughout all functional striatal territories and strongly influence the activity of striatal projection neurons (Graybiel, 1990; Bernacer et al., 2007; Pisani et al., 2007; Tepper et al., 2008; Ding et al., 2010; Bonsi et al., 2011; Crittenden and Graybiel, 2011). Their extensive dendritic and axonal arbors allow them to integrate and transmit information across functionally diverse striatal territories, subserving their known role in processing attentional salient stimuli in the context of reward-related behaviors (Kimura et al., 1984; Matsumoto et al., 2001; Pisani et al., 2001; Ravel et al., 2003; Morris et al., 2004; Joshua et al., 2008; Aosaki et al., 2010; Apicella et al., 2011; Bonsi et al., 2011).

Anatomical, electrophysiological, and neurochemical studies in rodents and primates have suggested that the excitability of ChIs is strongly modulated by GABAergic inputs (DiFiglia, 1987; Sullivan et al., 2008; Tepper et al., 2008; Ding et al., 2010; Bonsi et al., 2011; English et al., 2012). Although it is likely that most of these afferents originate from intrinsic striatal sources, including GABAergic interneurons and axon collaterals of striatal output neurons (Bolam et al., 1986, 2000; Martone et al., 1992; Tepper et al., 2004, 2008; Wilson, 2007), the relative abundance of these various GABAergic inputs upon ChIs is unknown. To address this issue, we quantitatively assessed the prevalence and relative distribution of GABAergic terminals onto ChIs in the monkey postcommissural putamen. Furthermore, to specifically examine the contribution of GABAergic axon collaterals from direct or indirect striatofugal neurons to this innervation, we quantified the synaptic relationships between substance P (SP)- or enkephalin (Enk)-containing terminals (representing terminals of the direct and indirect pathway, respectively) and ChIs. Our findings show that striatal ChIs are a major target of GABAergic terminals, and that many of these afferents originate from axon collaterals of direct and indirect striatal projection neurons.

Some of these data have been presented in abstract form (Gonzales et al., 2009, 2010, 2011).

Materials and Methods

Animals

Brain tissue from six adult (3–9 years old; 5–8 kg) female rhesus monkeys (*Macaca mulatta*) from the Yerkes National Primate Research Center colony was used in this study. At the time of sacrifice, these animals were deeply anesthetized with an overdose of

pentobarbital (100 mg/kg, i.v.) and transcardially perfusion-fixed with a cold oxygenated Ringer's solution and a fixative containing 0.1% glutaraldehyde and 4% paraformaldehyde in phosphate buffer (PB; 0.1 M, pH 7.4). All procedures were approved by the Institutional Animal Care and Use Committee at Emory University and conform to the U.S. National Institutes of Health Guide for the Care and Use of Laboratory Animals (Garber et al., 2010).

Tissue processing

After perfusion, the brains were removed from the skull, cut in 10-mm-thick blocks in the coronal plane, and stored in cold phosphate-buffered saline (PBS; 0.01 M, pH 7.4) until sectioning. A vibrating microtome was used to cut the blocks into serial 60-μm-thick coronal sections that were collected in an antifreeze solution (1.4% NaH_2PO_4-H_20, 2.6% Na_2HPO_4-$7H_2O$, 30% ethylene glycol, 30% glycerol dissolved in distilled water) and stored in a −20°C freezer. Prior to the immunocytochemical processing, the sections were placed into a 1% sodium borohydride/PBS solution for 20 minutes, followed by washes with PBS.

Primary antibodies

Sections from the postcommissural putamen were processed for light and electron microscopy immunoperoxidase localization of choline acetyl transferase (ChAT) or immunogold localization of SP, Leucine [Leu^5]- and Methionine [Met^5]-Enk, or GABA by using highly specific, well-characterized monoclonal and polyclonal antibodies (Table 1). Two ChAT antibodies were used in order to have primary antibodies raised in different species for the double immunocytochemical reactions.

In the SP and ChAT double-label experiments, we used rabbit polyclonal anti-ChAT antibodies. The specificity of this antiserum has been demonstrated through experiments showing that the overall pattern of immunostaining obtained with this antiserum is confined to brain areas known to express detectable levels of ChAT (German et al., 1985; Peterson et al., 1990; Smith ML et al., 1993, 1994), and that preadsorption immunohistochemical assays resulted in the reduction of ChAT staining in these regions (Shiromani et al., 1987, 1990; Smith et al., 1993; Holt et al., 1997). Furthermore, western blot analysis from human brain or placental tissue showed a distinct band at 68 kDa that corresponds to the molecular weight of enzymatically active ChAT (Bruce et al., 1985).

In double-label immunocytochemistry experiments with the rabbit anti-Enk antibodies, we used goat polyclonal anti-ChAT antibodies. The specificity of this antiserum has been demonstrated through western blot analysis in rat and human brain tissue (Karson et al., 1993). Control incubations from which the primary antibodies were omitted resulted in a complete lack of striatal cell body or fiber immunostaining (Holt et al., 1999). We found that the application of either of the two ChAT antisera on the tissue used in our study resulted in a pattern of staining that resembled that found in previous studies of ChAT immunoreactivity in nonhuman primates (Graybiel et al., 1986; DiFiglia, 1987; Bernacer et al., 2007).

Monoclonal antibodies against SP were used to identify the direct pathway MSN collaterals, whereas the indirect pathway MSN collaterals were identified with polyclonal antibodies against Met-Enk and Leu-Enk (Table 1). The specificity of the SP antibodies used in this study have been demonstrated by showing the equal displacement of labeled SP by five-, six-, and eight-amino acid COOH-terminal fragments of SP, as well as full-length SP, and by the specific binding of these antibodies with cell bodies and terminals located in well-defined SP-containing nuclei in the central nervous system (Cuello et al., 1979; Beach and McGeer, 1984; Bolam and Izzo, 1988; Smith et al., 1998; Reiner et al., 1999, Wolansky et al., 2007). The lack of tissue labeling following incubation with nonimmune rat serum or

primary antibodies preabsorbed with SP further confirmed the specificity of these antibodies (Cuello et al., 1979; Mai et al., 1986).

In order to maximize labeling of indirect (Enk-positive) pathway neurons, we used a cocktail of antibodies against Met- and Leu-Enk (Cuello, 1978; Brann and Emson, 1980; Del Fiacco et al., 1982; DiFiglia et al., 1982; Smith et al., 1998). The specificity of these antibodies was demonstrated by preincubation of the diluted antisera with various concentrations of peptides that resulted in a lack of immunoreactivity in the tissue (Elde et al., 1976; Williams and Dockray, 1983). In addition, we found an almost complete segregation of labeling for SP and Enk in the GPe and GPi, as previously described using other SP and Enk antibodies in the basal ganglia of rats, monkeys, and humans (see Results, Fig 5) (Haber and Elde, 1981; DiFiglia et al., 1982; Williams and Dockray, 1983; Beach and McGeer, 1984; Reiner et al., 1999).

Lastly, affinity-purified rabbit polyclonal antibodies against GABA-bovine serum albumin (BSA) were used to localize GABA-containing terminals in the putamen (Table 1). Details about the production, characterization, and specificity of this antiserum have been extensively described in previous studies (Hodgson et al., 1985; Somogyi and Hodgson, 1985; Smith et al., 1987). In brief, biochemical specificity tests with nitrocellulose paper strips and preadsorption of antibodies with excess of synthetic GABA demonstrated that these antibodies are highly specific for GABA and do not cross-react with related amino acids (Hodgson et al., 1985).

Single immunoperoxidase labeling for light microscopy (LM)

Sections from the postcommissural putamen were treated at room temperature (RT) with sodium borohydride for 20 minutes followed by a preincubation for 1 hour in a solution containing 1% normal horse serum or normal goat serum (NGS), 0.3% Triton-X-100, and 1% BSA in PBS. Sections were then incubated for 24 hours at RT in a solution containing goat anti-ChAT (1:100), rat anti-SP (1:100), or rabbit anti-Met/Leu-Enk (1:1,000) in 1% normal horse or goat serum, 0.3% Triton-X-100, and 1% BSA in PBS. On the following day, sections were thoroughly rinsed in PBS and then incubated in a PBS solution containing either (secondary) biotinylated horse anti-goat IgGs, goat anti-rat IgGs, or goat anti-rabbit IgGs (1:200; Vector, Burlingame, CA) combined with 1% normal horse or goat serum, 0.3% Triton-X-100, and 1% BSA for 90 minutes at RT. Sections were exposed to an avidin-biotinperoxidase complex (ABC; 1:100 [Vector] for 90 minutes followed by rinses in PBS and Tris buffer (50 mM; pH 7.6). Sections were then incubated within a solution containing 0.025% 3,3′-diaminobenzidine tetrahydrochloride (DAB; Sigma, St. Louis, MO), 10 mM imidazole, and 0.005% hydrogen peroxide in Tris buffer for 10 minutes at RT, rinsed with PBS, placed onto gelatin-coated slides, and coverslipped with Permount. Lastly, the sections were analyzed by using a Leica DMLB light microscope (Vienna, Austria) and photographed by using a ScanScope light microscope (Aperio Technologies, Vista, CA).

Preparation for electron microscopic (EM) observations

Single pre-embedding immunoperoxidase labeling for electron microscopy—

Sections were treated with a 1% sodium borohydride solution, placed in a cryoprotectant solution (PB 0.05 M, pH 7.4, 25% sucrose, and 10% glycerol), frozen at –80°C for 20 minutes each, before being returned to PBS-based solutions with decreasing gradients of cryoprotectant, and lastly, washed thoroughly in PBS. The tissue was then preincubated for 1 hour at RT in a solution containing PBS, 1% NGS, and 1% BSA, followed by a 48-hour incubation at 4°C in the primary antibody solution containing goat anti-ChAT with either rat anti-SP, or rabbit anti-Met/Leu-Enk antibodies in 1% NGS and 1% BSA in PBS. Sections were rinsed in PBS three times, incubated in a PBS solution containing 1% NGS, and 1%

BSA combined with secondary biotinylated horse anti-goat, goat anti-rat, or goat anti-rabbit IgGs (1:200; Vector), for 90 minutes at RT, rinsed in PBS, and then exposed to ABC and DAB as described above. After DAB exposure, the tissue was rinsed in PB (0.1 M, pH 7.4) and treated for 20 minutes with 1% OsO_4, returned to PB, and then dehydrated with decreasing concentrations of ethanol. To increase the tissue contrast at the electron microscope level, 1% uranyl acetate was added to the 70% ethanol solution for 35 minutes in the dark. After alcohol dehydration, sections were placed in propylene oxide and embedded in epoxy resin (Durcupan, Fluka, Buchs, Switzerland) for at least 12 hours, mounted onto slides, and placed in a 60°C oven for 48 hours (Smith and Bolam, 1992). Tissue samples from the postcommissural putamen were cut out of large, resin-embedded sections and fixed onto resin blocks, before being cut into 60-nm ultrathin sections (Leica Ultracut T2). These sections were mounted onto Pioloform-coated copper grids, stained with a lead citrate for 5 minutes, and then examined with an electron microscope (EM; model 1011, Jeol, Peabody, MA). Digital micrographs of immunoreactive elements were collected with a Gatan CCD camera (Model 785; Warrendale, PA) controlled by Digital Micrograph software (version 3.11.1).

Double post-embedding immunogold for GABA and pre-embedding immunoperoxidase for ChAT—The methods for post-embedding GABA immunostaining used in this study are similar to those described by Somogyi and Hodgson (1985) as modified by Phend et al. (1992). A series of adjacent ultrathin sections of striatal tissue immunostained with the goat anti-ChAT antibody (1:100 dilution) with the pre-embedding immunoperoxidase method mentioned above were cut with an ultramicrotome and placed onto gold grids. Once the grids were dry, they were preincubated in a solution containing Tris-buffered saline (TBS; 0.5 M, pH 7.6) and 0.01% Triton X-100 (TBS-T) and then, incubated overnight at RT with primary rabbit anti-GABA IgGs (1:1,000; Sigma) in TBS-T. On the next day, the grids were rinsed in a series of TBS-T washes, followed by a rinse in TBS (0.05 M, pH 8.2, 10 minutes,) and incubated with 15 nm gold-conjugated goat anti-rabbit IgG (1:50 in TBS 0.05 M, pH 8.2; British Biocell, Cardiff, UK, 90 minutes). The sections were then rinsed in TBS (0.05 M, pH 8.2) for 20 minutes, washed in distilled water for 5 minutes, and stained with 1% uranyl acetate (in distilled water, 90 minutes). Lastly, the grids were washed in distilled water and stained with lead citrate for 5 minutes before being examined with the electron microscope.

Double pre-embedding immunoperoxidase for ChAT and pre-embedding immunogold for SP or Met/Leu-Enk—Following sodium borohydride treatment, sections were processed with the cryoprotectant protocol described above followed by rinses in PBS and preincubation for 30 minutes in a PBS solution containing 5% dry milk. Sections were then rinsed in a TBS-gelatin buffer (0.02 M, 0.1% gelatin, pH 7.6), and incubated in an antibody solution (either rat anti-SP with rabbit anti-ChAT or rabbit anti-Met-/Leu-Enk with goat anti-ChAT) with 1% dry milk in TBS-gelatin buffer for 24 hours at RT. Additional control sections for each experiment were incubated in solutions from which either of the two primary antibodies was omitted in order to assess specificity of the immunogold and immunoperoxidase labeling. One day later, sections were rinsed in TBS-gelatin and then treated for 2 hours at RT with the following secondary antibody solutions prepared with TBS-gelatin in 1% milk. To visualize SP and ChAT, we used secondary goat anti-rat Fab′ fragments conjugated to 1.4-nm gold particles (1:100; Nanoprobes, Yaphank, NY) and secondary biotinylated goat anti-rabbit IgG (1:200; Vector), respectively. To visualize Met-/Leu-Enk and ChAT, we used secondary goat anti-rabbit Fab′ fragments conjugated to 1.4-nm gold particles (1:100; Nanoprobes) and secondary biotinylated horse anti-goat IgG (1:200; Vector). Sections were washed in TBS-gelatin and 2% sodium acetate buffer before incubation with the HQ Silver Kit (Nanoprobes) for 4–10 minutes to increase gold particle

sizes to 30–50 nm through silver intensification. Following this reaction and TBS-gelatin washes, ABC and DAB procedures were carried out as described above to localize ChAT.

Sections were rinsed in PB (0.1 M, pH 7.4) and treated with the same protocols for osmification, dehydration, embedding, and tissue selection described above, with the exception that sections were kept in 0.5% OsO_4 for 10 minutes, and the tissue was stained with 1% uranyl acetate for 10 minutes in the dark.

Analysis of material

GABA inputs onto ChAT-positive interneurons—To determine the proportion of GABA-positive terminals onto ChIs, ultrathin sections of double immunostained tissue (ChAT/GABA) from the postcommissural putamen of four animals were randomly examined to localize ChAT-immunoreactive (ir) dendrites and somata. A series of large-, medium-, and small-sized ChAT-positive dendrites were selected for this analysis (classification scheme described below), irrespective of their type and extent of synaptic innervation. We calculated an index of the density of gold particles in every terminal bouton that formed clearly identifiable symmetric or asymmetric synapses (Peters et al., 1991; Peters and Palay, 1996) with ChAT-positive elements, by dividing the number of gold particles for each individual terminal by the cross-sectional area of that terminal (Rasband, 1997–2012). A bouton was categorized as “symmetric/GABA-positive” if it formed a symmetric synapse, and if the gold particle density in the bouton was three times greater than the average gold particle density associated with terminals forming asymmetric synapses. Terminal boutons forming symmetric synapses that contained gold particle densities below this cutoff were categorized as “symmetric/unknown.” Because of interindividual variability in the absolute number of gold particles associated with GABA-positive and GABA-negative terminals across animals and postembedding reactions, these measurements were collected for each run of postembedding reaction in the striatal tissue from each monkey (Fig. 3E). Once the gold particle densities were measured for each individual animal, the mean percentage of the different subtypes of terminals in contact with different parts of ChAT-positive neurons was determined in that animal and compared across groups by using a one-way analysis of variance (ANOVA) with a post hoc Tukey's test (significance level set at $P < 0.05$; Fig. 4B).

SP or Met-/Leu-Enk-positive terminals onto ChAT-positive interneurons—Sections from the postcommissural putamen double-labeled with antibodies for rat anti-SP (gold-labeled) and goat anti-ChAT (peroxidase-labeled; five animals) or rabbit anti-Met-/Leu-Enk (gold-labeled) and goat anti-ChAT (peroxidase-labeled; four animals) were used to quantify the proportion of SP- or Enk-positive terminals in contact with ChAT-ir neurons. In order to avoid subjective bias, the tissue was randomly scanned for gold-labeled SP or Met-/Leu-Enk terminals and their postsynaptic target (i.e., ChAT-labeled or unlabeled) was determined irrespective of their possible association with ChAT-positive or ChAT-negative elements. The tissue was randomly scanned to determine the proportion of gold-labeled SP or Met-/Leu-Enk terminals that formed synapses with ChAT-ir neurons. The postsynaptic target of approximately 100 immunostained boutons per animal was categorized as ChAT-positive (or not) for each double-label experiment (Fig. 6F,G). The average proportion of SP- or Met/Leu-Enk-positive terminals forming synapses onto ChAT-labeled elements was compared by using Student's *t*-test (significance level set at $P < 0.05$; Fig. 6F) and between the postsynaptic targets within each group by using Student's *t*-test (significance level set at $P < 0.05$; Fig. 6G).

In order to ascertain whether the overall pattern of ChAT labeling was similar between series of double immunoreactions, we determined the relative density of ChAT-ir elements

in each block of tissue used from double immunostained sections. Ultrathin sections were also taken from tissue that was labeled for ChAT alone in one monkey to compare the overall pattern of ChAT immunoreactivity in this tissue with that found in the double-labeled material. To determine the density of ChAT-labeled elements in each of these tissue blocks, we took 25 digital micrographs of random tissue locations from the surface of the blocks at 25,000×. ChAT-ir elements were categorized as cell bodies, dendrites, or terminals, based on ultrastructural features described in Peters et al. (1991). The cross-sectional diameter of each dendrite was measured by using Image J (Rasband, 1997–2012), and dendritic profiles were categorized as large-sized (diameter > 0.99 μm, presumably representing proximal dendrites), medium-sized (diameter 0.5-0.99 μm), and small-sized (diameter < 0.5 μm, presumably representing distal dendrites) (DiFiglia and Carey, 1986; DiFiglia, 1987; Peters et al., 1991; Yelnik et al., 1991). The double-labeled sections were used for further quantification only if the proportion of ChAT-labeled proximal and distal dendrites were comparable to that in singly labeled sections (see Fig. 6E).

Total synaptic innervation of ChAT-positive neurons from SP- or ENK-positive terminals

In other measurements on the same double-immunostained striatal tissue in three monkeys, we determined the proportion of synaptic inputs onto ChIs accounted for by SP- or Enk-positive terminals. To do so, we characterized the synaptic innervation of approximately 100 ChAT-containing dendrites in each animal. The percentage of total boutons in contact with these dendrites was categorized as follows: 1) symmetric/SP-positive or symmetric/Enk-positive; 2) symmetric/SP-negative or symmetric/Enk-negative; and 3) asymmetric/SP-negative or asymmetric/Enk-negative. The results were then statistically analyzed with a Student's *t*-test (significance set at $P < 0.05$) (Fig. 7B,C).

In order to ensure that the quantitative analysis of the double-labeled material was not affected by poor tissue penetration of antibodies or gold particles, we compared the density of SP-and Enk-ir boutons in the single-labeled (immunoperoxidase) and double-labeled (immunogold) tissue, with the expectation that they would be in the same range. For this analysis, single- or double-labeled ultrathin sections from the surface of blocks with suitable ultrastructural preservation were randomly scanned for areas of tissue that had terminal immunostaining for SP or Met-/Leu-Enk, and electron micrographs were taken of every field visible in that area at 25,000×. To calculate the bouton density index, the number of labeled terminals in these micrographs was counted and divided by the total surface area represented by the examined micrographs. If the density of labeled boutons in the double-labeled tissue was 10% lower than that calculated in single-labeled sections, the tissue was not considered for further analysis.

Results

GABAergic inputs onto cholinergic interneurons

At the light microscopic level, the neuropil in the caudate nucleus and putamen was moderately immunoreactive, consisting of a meshwork of fine ChAT-labeled processes and large immunoreactive cell bodies with prominent primary dendritic shafts from which emerged thinner dendritic processes that often extended over long distances from their parent cell bodies (Fig. 1). These morphological characteristics are consistent with those described for ChAT-positive neurons in previous primate studies (DiFiglia, 1987; Bernacer et al., 2007).

The GABAergic innervation of cholinergic cells was characterized from postcommissural putamen tissue that was double immunostained for ChAT (pre-embedding immunoperoxidase) and GABA (postembedding immunogold). At the electron microscopic

level, ChAT-immunostained cell bodies, dendrites, and axon terminals displayed the electron-dense amorphous DAB reaction product (Fig. 2), whereas GABA-ir terminals were recognized by their large density of gold particles (Fig. 2A,B). To assess the specificity of the immunogold reaction for GABA, we analyzed the relative density of gold particles associated with terminals forming symmetric (putatively GABAergic) or asymmetric (putatively glutamatergic) synapses in the double-immunostained striatal tissue (Fig. 3). We performed this analysis separately for each of the four animals used in this part of the study (animals 1–4 in Fig. 3), because the absolute number of gold particles over labeled and unlabeled elements across animals may vary when localized with the postembedding immunogold method. In each animal, the average density of gold particles associated with terminals forming symmetric synapses outnumbered that in terminals forming asymmetric synapses (Figs. 2, 3) by a factor of 4:1 (Fig. 3E). As described in Materials and Methods, we used these data to categorize the neurochemical phenotype of terminals forming synapses onto ChAT-positive elements. As shown in Figure 4A, the analysis of a total of 709 afferent terminals in synaptic contact with ChAT-ir profiles (soma = 26; large-sized dendrites = 133; medium-sized dendrites = 328; small-sized dendrites = 222) revealed that 60 ± 4% were GABAergic, 19 ± 4% were categorized as symmetric/unknown, and 21 ± 4% were asymmetric/non-GABAergic (putatively glutamatergic).

When the postsynaptic ChAT-ir elements were categorized as soma or dendrites of various sizes based on their cross-sectional diameter, the medium-sized (0.5–0.99 μm in diameter) and large-sized (diameter > 0.99 μm) dendrites received a significantly greater proportion of synaptic inputs from symmetric GABAergic boutons (N terminals = 418; 29 ± 1% and 13 ± 2% of total synapses onto ChAT-positive elements, respectively) than from the symmetric unknown (N terminals = 137; 10 ± 2% and 4 ± 1%, respectively) and asymmetric non-GABAergic boutons (N terminals = 155; 7 ± 2% and 1 ± 0.3%, respectively) ($P < 0.001$, one-way ANOVA with a post hoc Tukey's test; Fig. 4B). A significant difference was also found between the percentage of symmetric GABAergic inputs versus symmetric unknown inputs onto small (<0.5 μm in diameter) ChAT-positive dendrites ($P < 0.001$, one-way ANOVA with a post hoc Tukey's test; Fig. 4B).

“Direct” and “indirect” striatofugal inputs onto cholinergic interneurons— Experiments were carried out to determine the proportion of GABAergic inputs onto ChAT-labeled neurons that originate from axon collaterals of striatal projection neurons. To do so, we took advantage of the segregation of SP and Enk into two populations of striatofugal neurons to label GABAergic terminals that originate from direct or indirect pathway projection neurons, respectively (Brann and Emson, 1980; Cuello et al., 1981; Del Fiacco et al., 1982; Beach and McGeer, 1984; Reiner et al., 1999). In agreement with previous reports (Haber and Elde, 1981; DiFiglia et al., 1982; Williams and Dockray, 1983; Beach and McGeer, 1984; Reiner et al., 1999), the striatum and GPi showed strong positive immunostaining for SP (Fig. 5A), whereas the antibodies for Met-/Leu-Enk positively labeled the striatum and GPe (Fig. 5B,C).

In double-label experiments, the pre-embedding immunogold method was used to localize SP or Enk immunoreactivity, whereas ChAT-positive neurons were labeled with the immunoperoxidase method (Fig. 6A–D). Consistent with previous reports on the ultrastructural localization of SP and Enk immunoreactivity in the primate striatum (DiFiglia et al., 1982; Hutcherson and Roberts, 2005), most immunoreactivity was found in terminals forming symmetric synapses. Less labeling was observed in dendrites, cell bodies, and dendritic spines (Fig. 6A–D). Gold-containing boutons were only considered as being positively labeled if they contained two or more gold particles. The gold particles were often found in large densecore vesicles, a known vesicular storage site of neuropeptides in central nervous system (CNS) neurons (Merighi et al., 2011) (Fig. 6A–D). The pattern of ChAT

immunostaining in the double-labeled tissue was the same as described above for the ChAT/GABA-immunostained material (Fig. 6E). Very few neuronal elements exhibited dual labeling for gold and peroxidase in the double-immunostained material, indicating the lack of SP/ChAT or Enk/ChAT colocalization (Fig. 6A–D).

SP-positive inputs onto ChAT-immunoreactive neurons

In the first series of double-label experiments carried out using postcommissural putamen tissue from five monkeys, the proportion of SP-positive terminals in contact with ChAT-labeled neurons was determined. Ultrathin sections taken from the surface of blocks of striatal tissue that contained elements labeled with either gold (i.e., SP-positive) or peroxidase (i.e., ChAT-positive) deposits were examined to determine whether the postsynaptic targets of SP-ir elements contained ChAT immunoreactivity. The analysis of 527 SP-ir terminals revealed that 36 ± 4% of these boutons formed symmetric synapses with ChAT-ir dendrites (Fig. 6A,B), which were preferentially of the medium (52 ± 6%) or small (29 ± 3%) size diameter (Fig. 6G).

We also determined the proportion of the total synaptic innervation of ChAT-positive neurons that was accounted for by SP-ir terminals in three of the five monkeys used in the previous analysis. In areas that contained both gold-and peroxidase-labeled structures, the tissue was randomly scanned under the electron microscope for ChAT-ir dendrites. The analysis of 219 ChAT-ir dendrites (large-sized = 21; medium-sized = 140; small-sized = 58) revealed that 16 ± 1% of their total synaptic innervation was from SP-ir terminals forming symmetric synapses, whereas 68 ± 3% originated from SP-negative boutons forming symmetric synapses (Fig. 7B), and 16 ± 2% came from putatively glutamatergic terminals forming asymmetric synapses (Fig 7B). The proportion of SP-negative terminals forming symmetric synapses (i.e., Symm/SP(−)) with medium-sized ChAT-labeled dendrites was significantly larger than the two other populations of terminals in contact with these ChAT-positive elements (Fig. 7B). To ensure that the overall density of gold-containing SP-ir terminals in the putamen of monkeys used in these double-label reactions (n = 3) was not underestimated because of the double-labeling procedure, we compared it with the density of SP-ir boutons found in single SP-labeled sections processed with the immunoperoxidase reaction (n = 1; Fig. 7A). We found that these values were in the same range, thereby showing that our results were not affected by a limited penetration of the gold-conjugated secondary antibodies used to label SP in this tissue.

Enk-positive terminals onto ChAT-positive neurons

In the other series of double-label experiments, we studied the synaptic relationships between Enk-positive terminals and ChAT-ir elements in the postcommissural putamen of four of the five animals that were used for the SP/ChAT analysis described in the previous section. The analysis of 454 Enk-positive terminals revealed that 47 ± 2% of these terminals formed symmetric synapses with ChAT-positive dendrites and soma (Fig. 6F), a proportion significantly greater ($P < 0.05$, Student's *t*-test) than that found for SP-positive terminals in contact with ChAT-positive cells (Fig. 6F). This difference is accounted for by a significantly larger proportion of Enk-ir terminals in contact with large ChAT-positive dendrites (Fig. 6G; $P = 0.012$; Student's *t*-test).

In the same material, the analysis of the synaptic innervation of 208 ChAT-positive dendrites (large-sized = 45; medium-sized =118; small-sized = 45) revealed that 11 ± 1% of all boutons forming synapses with ChAT-positive dendrites were immunoreactive for Enk, whereas 79 ± 3% and 10 ± 1% of the total synaptic innervation of ChAT-containing dendrites was accounted for by Enk-negative symmetric or asymmetric synapses, respectively (Fig. 7C). Large- and medium-sized ChAT-positive dendrites received a

significantly larger synaptic innervation from Enk-negative boutons forming symmetric synapses (i.e., Symm/Enk(−)) than from symmetric Enk-positive and asymmetric Enk-negative terminals ($P < 0.001$, one-way ANOVA with a post hoc Tukey's test; Fig. 7C). In contrast, small-sized ChAT-ir dendrites also received a significantly greater synaptic innervation from the symmetric Enk-negative terminals than the symmetric Enk-positive terminals ($P < 0.001$, oneway ANOVA with a post hoc Tukey's test; Fig. 7C), but it did not reach significance when compared with putatively glutamatergic boutons (i.e., Asymm/Enk(−)). As was the case for the SP/ChAT double immunostaining, the average relative density of gold-containing Enk-positive terminals seen in our double-immunostained tissue was the same as that assessed in striatal sections single-stained for Enk by using the immunoperoxidase method (Fig. 7A).

Altogether, findings from the double-immunostaining striatal sections for SP or Enk with ChAT revealed that 24 ± 1% of the total synaptic innervation of ChIs in the monkey postcommissural putamen originate from axon collaterals of GABAergic direct and indirect striatal projection neurons, whereas 63 ± 2% arise from other subpopulations of terminals that form symmetric synapses, and 13 ± 2% from putatively glutamatergic boutons (Figs. 7D, 8).

Discussion

Our findings demonstrate that ChIs are a major target of GABAergic inputs, and that a significant proportion of this innervation originates from axon collaterals of direct and indirect medium spiny projection neurons in the monkey postcommissural putamen. Through these anatomical connections, the intrinsic axon collaterals of GABAergic striatal projection neurons may exert a powerful control of ChI activity in primates.

Synaptic GABAergic regulation of striatal cholinergic interneurons

It is believed that the feedforward and feedback connections between intrinsic striatal GABAergic neurons and ChIs (DiFiglia, 1987; Sullivan et al., 2008; Tepper et al., 2008; Ding et al., 2010; Bonsi et al., 2011; English et al., 2012) may play a role in behaviors such as attention and reward-based learning (Kimura et al., 1984; Matsumoto et al., 2001; Ravel et al., 2003; Morris et al., 2004; Joshua et al., 2008; Aosaki et al., 2010; Apicella et al., 2011; Bonsi et al., 2011). Many in vitro studies have characterized the synaptic influences of intrastriatal GABAergic connections on the excitability and/or spontaneous activity of cholinergic cells in rodents. For example, activation of $GABA_A$ receptors, located postsynaptically on ChIs (DeBoer and Westerink, 1994; Yan and Surmeier, 1997; Fujiyama et al., 2000; Waldvogel et al., 2004), readily evoked inhibitory postsynaptic potentials (IPSPs) in tonically active neurons (TANs) (Yan and Surmeier, 1997; Bennett and Wilson, 1998; Pisani et al., 2000), and decreased striatal acetylcholine release (Anderson et al., 1993; DeBoer and Westerink, 1994) in rodents.

Previous electron microscopic studies in rodents and monkeys have shown that most synaptic inputs to the somatodendritic domain of ChIs are symmetric (Chang and Kitai, 1982; Bolam et al., 1984; Phelps et al., 1985; DiFiglia, 1987; Sizemore et al., 2010). Although it is frequently assumed that such symmetric synapses are GABAergic (Gerfen, 1988; Pasik et al., 1988; Ribak and Roberts, 1990; Roberts et al., 1996), the chemical composition of terminals that form symmetric synapses in the striatum is heterogeneous, including, for instance, GABAergic, dopaminergic and cholinergic terminals (Haber, 1986; Semba et al., 1987; Gerfen, 1988; Graybiel, 1990; Smith Y et al., 1994; Bolam et al., 2000; Tepper et al., 2010; Crittenden and Graybiel, 2011).

Our data collected from material immunostained for GABA and ChAT provide direct ultrastructural evidence that most synaptic inputs onto ChIs in the monkey post-commissural putamen are, in fact, GABAergic. This pattern of synaptic connectivity is strikingly different from that of projection neurons, which receive most of their dendritic innervation from glutamatergic and dopaminergic inputs, except for the proximal somatodendritic domain that is innervated by GABAergic afferents from interneurons (Sadikot et al., 1992a,b; Bolam et al., 2000; Kubota and Kawaguchi, 2000; Wilson, 2007). The GABAergic inputs onto ChIs may originate from a variety of sources, including GABAergic collaterals of striatal projection neurons (Oertel et al., 1983; Aronin et al., 1984; Bradley et al., 1984; Christensson-Nylander et al., 1986; Penny et al., 1986; Surmeier et al., 1988; Graybiel, 1990; Bolam et al., 2000; Wilson, 2007), GABAergic parvalbumin- and calretinin-containing interneurons (Augood et al., 1995; Kawaguchi et al., 1997; Bolam et al., 2000; Kubota and Kawaguchi, 2000; Tepper et al., 2010), or extrinsic GABAergic inputs from the GPe (Beckstead, 1983; Oertel et al., 1984; Smith et al., 1987; Kita and Kitai, 1991; Bevan et al., 1998; Kita et al., 1999; Sato et al., 2000; Mallet et al., 2012). The prevalence of these respective inputs onto ChIs cells remains to be established. As discussed below, MSN axon collaterals are a significant source of this innervation.

It is noteworthy that a significant proportion of terminals involved in symmetric synaptic connections with ChIs did not, however, display a level of GABA immunoreactivity high enough to be categorized as GABAergic. The most likely source of these terminals may be the striatal neuropeptide-Y/somatostatin-containing interneurons, known to express a low level of GABA (Aoki and Pickel, 1989; Chesselet and Robbins, 1989; Vuillet et al., 1992; Kubota et al., 1993; Catania et al., 1995; Kubota and Kawaguchi, 2000). However, low levels of nonspecific gold labeling in dopaminergic SNc inputs (Kubota et al., 1987; Pickel and Chan, 1990; Dimova et al., 1993) or cholinergic terminals from striatal ChIs themselves (Calabresi et al., 1998; Sullivan et al., 2008) are other potential sources of these boutons.

Finally, we found that the distal dendrites of ChIs receive a significant innervation from putative glutamatergic terminals that form asymmetric synapses. Some of these terminals may originate from the cerebral cortex (Dub et al., 1988; Lapper and Bolam, 1992; Sadikot et al., 1992a; Dimova et al., 1993; Bennett and Wilson, 1998; Sidibe and Smith, 1999; Thomas et al., 2000), although most of them are likely to arise from projections of the centromedian/parafascicular thalamic nuclei (Meredith and Wouterlood, 1990; Lapper and Bolam, 1992; Bennett and Wilson, 1998; Sidibe and Smith, 1999).

Although the functional effects of GABAergic and putatively glutamatergic afferents on the activity of ChIs do not merely rely on their preferential distribution along the proximal and distal dendrites of these neurons, respectively, it is important to note that synaptic inputs onto primary dendrites are often seen as more powerful than distal synaptic afferents (Wilson, 2007). Thus, the pattern of synaptic organization of GABAergic and putatively glutamatergic inputs onto ChIs described in our study suggests that primate ChIs may be more strongly regulated by GABAergic than by glutamatergic inputs (Bennett and Wilson, 1998; Wilson, 2007; Tepper et al., 2008). However, rodent and monkey in vitro and in vivo electrophysiological data suggest that GABAergic and glutamatergic inputs to ChIs do not compete with one another but tend to be active in sequence. For instance, activation of glutamatergic inputs from the cerebral cortex or the thalamus often result in an early, presumably monosynaptic, excitation of ChIs, followed by a robust inhibition, which may be mediated by GABAergic intrastriatal axon collaterals or interneurons (Matsumoto et al., 2001; Suzuki et al., 2001; Reynolds and Wickens, 2004; Nanda et al., 2009; Ding et al., 2010). It is noteworthy that additional phenomena not studied here, such as spike back-propagation, dendritic calcium entry, or the type and density of postsynaptic receptors, may also contribute significantly to the synaptic strength of GABAergic and glutamatergic

synapses onto ChIs, as they do in striatal projection neurons (Banks et al., 1998; Kerr and Plenz, 2002, 2004; Plenz, 2003; Carter and Sabatini, 2004; Tepper and Bolam, 2004; Wilson, 2007; Day et al., 2008; English et al., 2012).

Axon collaterals of striatal projection neurons are a main source of GABAergic inputs to striatal cholinergic interneurons

We found that ChIs receive massive GABAergic inputs, but the exact source(s) of these afferents could not be determined solely based on GABA immunoreactivity. DiFiglia and Carey (1986) recognized up to eight morphologically different types of terminals forming symmetric synapses with ChIs, implying that these neurons receive GABAergic innervation from multiple sources. The phenotype of these neuronal sources can be identified by staining for neuropeptides and neurochemicals that coexist with GABA in these cells (Oertel et al., 1983; Aronin et al., 1984; Bradley et al., 1984; Christensson-Nylander et al., 1986; Penny et al., 1986; Surmeier et al., 1988), while not being significantly expressed in other striatal neurons or extrinsic afferents (Taniyama et al., 1980; Fonnum et al., 1981; Young et al., 1981; Kosaka et al., 1988; Kawaguchi et al., 1997; Kubota and Kawaguchi, 2000). In this study, we used the neuropeptides SP and Enk as markers of intrinsic axon collaterals of the two populations of striatal projection neurons (Cuello, 1978; Cuello et al., 1979; Brann and Emson, 1980; Del Fiacco et al., 1982; DiFiglia et al., 1982; Beach and McGeer, 1984; Smith et al., 1998; Reiner et al., 1999). Previous rodent studies have provided qualitative evidence that SP-expressing terminals form symmetric synapses with the somatodendritic domain of ChAT-labeled neurons (Bolam et al., 1986; Martone et al., 1992; Kuramoto et al., 2007). However, attempts at providing evidence for Enk- or parvalbumin-containing inputs onto ChIs in rats resulted in negative data (Chang and Kita, 1992; Martone et al., 1992), suggesting specific interactions between ChIs and the direct pathway MSNs.

In striking contrast with these studies, we found that 35.6% of SP-positive terminals and 47% Enk-labeled boutons form symmetric synapses with ChI dendrites in monkeys, indicating that ChIs are a major target of intrinsic axon collaterals of both direct and indirect pathway GABAergic MSNs in the primate postcommissural putamen. This discrepancy may be explained, in part, by the fact that the proportion of interneurons over the total striatal neuronal population is much larger in primates than in rodents (24% vs. approximately 5%; see Pasik et al., 1976; Graveland and DiFiglia, 1985; Roberts et al., 1996; Wu and Parent, 2000), and that striatal ChIs in primates have a denser and larger dendritic tree than rodents (DiFiglia et al., 1980; Bolam et al., 1984; Phelps et al., 1985; DiFiglia and Carey, 1986; Yelnik et al., 1991, 1993; Bernacer et al., 2007). Technical differences cannot be ruled out, especially the increased sensitivity of the ultrastructural double immunocytochemical technique used in our study. In regard to the SP innervation, although there appears to be a significant synaptic interaction between SP-positive terminals and ChIs in rodents, the supporting evidence for such connections is qualitative, making these findings difficult to compare with our quantitative data (Bolam et al., 1986; Kuramoto et al., 2007).

It is important to realize that our data lay the foundation for a potentially important, but unexplored, function of the local MSN axon collaterals. Although it has long been believed that these collaterals primarily reach other MSNs, it is now clear that these inter-MSN connections are sparse and confined to their distal dendrites, so that their functional impact is likely to be weak (Jaeger et al., 1994; Stern et al., 1998; Czubayko and Plenz, 2002; Tunstall et al., 2002; Tecuapetla et al., 2005; Wilson, 2007; Blomeley and Bracci, 2008, 2011; Taverna et al., 2008; Tepper et al., 2008; Blomeley et al., 2009). Our findings suggest that one of the main targets of MSN collaterals in primates could instead be ChIs, and that such interactions could permit MSNs to regulate the activity of ChIs.

Peptidergic modulation of ChIs by striatal projection neurons?

In addition to their GABAergic influences, MSN collaterals could also modulate the activity of ChIs through the release of their coexpressed neuropeptides, SP and Enk. It has, indeed, been shown that these neuropeptides participate in the synaptic modulation of striatal neuronal activity (Aosaki and Kawaguchi, 1996; Miura et al., 2007, 2008; Blomeley et al., 2009; Govindaiah et al., 2010; Merighi et al., 2011). Thus, in vitro and in vivo studies have demonstrated that SP and Enk are released in the striatum (Lindefors et al., 1985, 1989; Llorens-Cortes et al., 1990; Ruzicka et al., 1991; Bell et al., 1998; Jabourian et al., 2004). In addition, rat and primate ChIs display strong mRNA and protein expression for tachykinin NK1 receptors (Gerfen et al., 1991; Kaneko et al., 1993; Aubry et al., 1994; Parent et al., 1995; Richardson et al., 2000; Perez et al., 2007) along with mu- and delta-opioid receptors (Pasquini et al., 1992; Lendvai et al., 1993; Le Moine et al., 1994; Jabourian et al., 2005; Perez et al., 2007), which, upon activation, lead to an increase or decrease in the striatal acetylcholine (ACh) release, respectively (Mulder et al., 1984; De Vries et al., 1989; Lapchak et al., 1989; Izquierdo, 1990; Arenas et al., 1991; Lendvai et al., 1993; Perez et al., 2007). In vitro studies from rat brain slices demonstrated that the release of striatal SP from MSN axon collaterals, or bath-applied SP, leads to the depolarization of TANs, but not fast-spiking interneurons or other MSNs (Aosaki and Kawaguchi, 1996; Kawaguchi et al., 1997; Bell et al., 1998; Govindaiah et al., 2010), whereas Enk activation of opioid receptors results in the hyperpolarization of ChIs (Jiang and North, 1992; Miura et al., 2007). Therefore, the prominent synaptic interactions between SP-positive and Enk-positive terminals and cholinergic neurons shown in our study also open up the possibility for peptidergic modulation of primate ChIs.

Conclusions

The strong association between MSNs and ChIs shown in this study provides further evidence that the reciprocal functional interactions between these two neuronal populations are important elements of striatal processing. Cholinergic modulation of MSNs has long been established (Phelps et al., 1985; DiFiglia, 1987; Izzo and Bolam, 1988; Graybiel, 1990; Pisani et al., 2007; Tepper et al., 2008), but the exact role(s) of MSN-ChI connections remains to be determined. It is possible, however, that an additional role of striatal ChIs, besides feedback modulation of directly coupled MSNs, is to provide feed-forward information from one group of MSNs to another through MSN-ChI-MSN chains. In primates, such links may exist between direct and indirect striatofugal neurons situated in functionally specific striatal territories or between MSNs located in striatal patch and matrix compartments, supported by the fact that cholinergic cell bodies are often located along the borders of striatal patches, whereas their dendrites extend beyond the boundaries of each striatal compartment (Graybiel et al., 1986; Kubota and Kawaguchi, 1993; Aosaki et al., 1995; Kawaguchi et al., 1995; Bernacer et al., 2007).

Interactions between MSNs and ChIs may also be relevant in disease states, specifically in those known to respond to cholinergic medications, such as Parkinson's disease or dystonia (Pisani et al., 2007; Bonsi et al., 2011; Goldberg et al., 2012). Although the functional significance of MSN-ChI neuron connections under normal or diseased states remains poorly understood, it is noteworthy to mention that the metabolic and physiological activity of both populations of MSNs, as well as MSN-MSN synaptic interconnections, are significantly altered in the dopamine-depleted state (Ingham et al., 1991; Taverna et al., 2008; Surmeier, 2010; Gerfen and Surmeier, 2011). The overall firing frequency of striatal ChIs does not change in parkinsonism (Raz et al., 1996, 2001; Aosaki et al., 2010). However, significant abnormal cholinergic function in the dopamine-depleted striatum has been noted (Pisani et al., 2007; Bonsi et al., 2011; Goldberg et al., 2012), but may not be solely dependent upon the removal of dopamine from the system (MacKenzie et al., 1989;

Joyce, 1991, 1993; Ding et al., 2006). Thus, in light of our data showing that inputs from MSN collaterals are located to subserve control over ChIs, a detailed characterization of the electrophysiological properties of MSN-ChI synaptic connections in normal and parkinsonian states is warranted.

Acknowledgments

The authors thank Susan Jenkins for her excellent assistance with immunohistochemical matters and electron microscopy and Dr. Adriana Galvan for critical reading of the manuscript. We also thank Alex Derienko from Emory Graphic Design Service for his elegant illustration used in Figure 8 of this paper.

National Institute of Health R01NS037948 (YS, TW), R01NS062876 (TW,YS), P50NS071669 (TW,YS) and F31NS066754 (KKG). NIH base grant to the Yerkes National Primate Research Center (RR00165).

Literature Cited

Albin RL, Young AB, Penney JB. The functional anatomy of basal ganglia disorders. Trends Neurosci. 1989; 12:366–375. [PubMed: 2479133]

Alexander GE, Crutcher MD, DeLong MR. Basal gangliathalamocortical circuits: parallel substrates for motor, oculomotor, “prefrontal” and “limbic” functions. Prog Brain Res. 1990; 85:119–146. [PubMed: 2094891]

Anderson JJ, Kuo S, Chase TN, Engber TM. GABAA and GABAB receptors differentially regulate striatal acetylcholine release in vivo. Neurosci Lett. 1993; 160:126–130. [PubMed: 8247341]

Aoki C, Pickel VM. Neuropeptide Y in the cerebral cortex and the caudate-putamen nuclei: ultrastructural basis for interactions with GABAergic and non-GABAergic neurons. J Neurosci. 1989; 9:4333–4354. [PubMed: 2687439]

Aosaki T, Kawaguchi Y. Actions of substance P on rat neostriatal neurons in vitro. J Neurosci. 1996; 16:5141–5153. [PubMed: 8756443]

Aosaki T, Kimura M, Graybiel AM. Temporal and spatial characteristics of tonically active neurons of the primate's striatum. J Neurophysiol. 1995; 73:1234–1252. [PubMed: 7608768]

Aosaki T, Miura M, Suzuki T, Nishimura K, Masuda M. Acetylcholine-dopamine balance hypothesis in the striatum: an update. Geriatr Gerontol Int. 2010; 10(suppl 1):S148–157. [PubMed: 20590830]

Apicella P, Ravel S, Deffains M, Legallet E. The role of striatal tonically active neurons in reward prediction error signaling during instrumental task performance. J Neurosci. 2011; 31:1507–1515. [PubMed: 21273435]

Arenas E, Alberch J, Perez-Navarro E, Solsona C, Marsal J. Neurokinin receptors differentially mediate endogenous acetylcholine release evoked by tachykinins in the neostriatum. J Neurosci. 1991; 11:2332–2338. [PubMed: 1651375]

Aronin N, Difiglia M, Graveland GA, Schwartz WJ, Wu JY. Localization of immunoreactive enkephalins in GABA synthesizing neurons of the rat neostriatum. Brain Res. 1984; 300:376–380. [PubMed: 6375810]

Aubry JM, Lundstrom K, Kawashima E, Ayala G, Schulz P, Bartanusz V, Kiss JZ. NK1 receptor expression by cholinergic interneurones in human striatum. Neuroreport. 1994; 5:1597–1600. [PubMed: 7819527]

Augood SJ, Herbison AE, Emson PC. Localization of GAT-1 GABA transporter mRNA in rat striatum: cellular coexpression with GAD67 mRNA, GAD67 immunoreactivity, and parvalbumin mRNA. J Neurosci. 1995; 15:865–874. [PubMed: 7823186]

Banks MI, Li TB, Pearce RA. The synaptic basis of GABAA, slow. J Neurosci. 1998; 18:1305–1317. [PubMed: 9454840]

Beach TG, McGeer EG. The distribution of substance P in the primate basal ganglia: an immunohistochemical study of baboon and human brain. Neuroscience. 1984; 13:29–52. [PubMed: 6208509]

Beckstead RM. A pallidostriatal projection in the cat and monkey. Brain Res Bull. 1983; 11:629–632. [PubMed: 6661668]

Bell MI, Richardson PJ, Lee K. Characterization of the mechanism of action of tachykinins in rat striatal cholinergic interneurons. Neuroscience. 1998; 87:649–658. [PubMed: 9758231]

Bennett BD, Wilson CJ. Synaptic regulation of action potential timing in neostriatal cholinergic interneurons. J Neurosci. 1998; 18:8539–8549. [PubMed: 9763496]

Bernacer J, Prensa L, Gimenez-Amaya JM. Cholinergic interneurons are differentially distributed in the human striatum. PLoS ONE. 2007; 2:e1174. [PubMed: 18080007]

Bevan MD, Booth PA, Eaton SA, Bolam JP. Selective innervation of neostriatal interneurons by a subclass of neuron in the globus pallidus of the rat. J Neurosci. 1998; 18:9438–9452. [PubMed: 9801382]

Blomeley C, Bracci E. Substance P depolarizes striatal projection neurons and facilitates their glutamatergic inputs. J Physiol. 2008; 586:2143–2155. [PubMed: 18308827]

Blomeley CP, Bracci E. Opioidergic interactions between striatal projection neurons. J Neurosci. 2011; 31:13346–13356. [PubMed: 21940429]

Blomeley CP, Kehoe LA, Bracci E. Substance P mediates excitatory interactions between striatal projection neurons. J Neurosci. 2009; 29:4953–4963. [PubMed: 19369564]

Bolam JP, Izzo PN. The postsynaptic targets of substance P-immunoreactive terminals in the rat neostriatum with particular reference to identified spiny striatonigral neurons. Exp Brain Res. 1988; 70:361–377. [PubMed: 2454839]

Bolam JP, Wainer BH, Smith AD. Characterization of cholinergic neurons in the rat neostriatum. A combination of choline acetyltransferase immunocytochemistry, Golgi-impregnation and electron microscopy. Neuroscience. 1984; 12:711–718. [PubMed: 6382048]

Bolam JP, Ingham CA, Izzo PN, Levey AI, Rye DB, Smith AD, Wainer BH. Substance P-containing terminals in synaptic contact with cholinergic neurons in the neostriatum and basal forebrain: a double immunocytochemical study in the rat. Brain Res. 1986; 397:279–289. [PubMed: 2432992]

Bolam JP, Hanley JJ, Booth PA, Bevan MD. Synaptic organisation of the basal ganglia. J Anat. 2000; 196:527–542. [PubMed: 10923985]

Bonsi P, Cuomo D, Martella G, Madeo G, Schirinzi T, Puglisi F, Ponterio G, Pisani A. Centrality of striatal cholinergic transmission in basal ganglia function. Front Neuroanat. 2011; 5:6. [PubMed: 21344017]

Bradley RH, Kitai ST, Wu JY. An immunocytochemical analysis of methionine enkephalin, substance P, and glutamic acid decarboxylase within neostriatal neurons. J Am Osteopath Assoc. 1984; 84(1 suppl):98–110. [PubMed: 6208175]

Brann MR, Emson PC. Microiontophoretic injection of fluorescent tracer combined with simultaneous immunofluorescent histochemistry for the demonstration of efferents from the caudate-putamen projecting to the globus pallidus. Neurosci Lett. 1980; 16:61–65. [PubMed: 6189003]

Bruce G, Wainer BH, Hersh LB. Immunoaffinity purification of human choline acetyltransferase: comparison of the brain and placental enzymes. J Neurochem. 1985; 45:611–620. [PubMed: 4009177]

Calabresi P, Centonze D, Pisani A, Sancesario G, North RA, Bernardi G. Muscarinic IPSPs in rat striatal cholinergic interneurones. J Physiol. 1998; 510:421–427. [PubMed: 9705993]

Carter AG, Sabatini BL. State-dependent calcium signaling in dendritic spines of striatal medium spiny neurons. Neuron. 2004; 44:483–493. [PubMed: 15504328]

Catania MV, Tölle TR, Monyer H. Differential expression of AMPA receptor subunits in NOS-positive neurons of cortex, striatum, and hippocampus. J Neurosci. 1995; 15:7046–7061. [PubMed: 7472460]

Chang HT, Kitai ST. Large neostriatal neurons in the rat: an electron microscopic study of gold-toned Golgi-stained cells. Brain Res Bull. 1982; 8:631–643. [PubMed: 6182960]

Chang HT, Kita H. Interneurons in the rat striatum: relationships between parvalbumin neurons and cholinergic neurons. Brain Res. 1992; 574:307–311. [PubMed: 1638402]

Chesselet MF, Robbins E. Characterization of striatal neurons expressing high levels of glutamic acid decarboxylase messenger RNA. Brain Res. 1989; 492:237–244. [PubMed: 2568874]

Christensson-Nylander I, Herrera-Marschitz M, Staines W, Hökfelt T, Terenius L, Ungerstedt U, Cuello C, Oertel WH, Goldstein M. Striato-nigral dynorphin and substance P pathways in the rat.

I. Biochemical and immunohistochemical studies. Exp Brain Res. 1986; 64:169–192. [PubMed: 2429858]

Crittenden JR, Graybiel AM. Basal ganglia disorders associated with imbalances in the striatal striosome and matrix compartments. Front Neuroanat. 2011; 5:59. [PubMed: 21941467]

Cuello AC. Endogenous opioid peptides in neurons of the human brain. Lancet. 1978; 2:291–293. [PubMed: 79085]

Cuello AC, Galfre G, Milstein C. Detection of substance P in the central nervous system by a monoclonal antibody. Proc Natl Acad Sci U S A. 1979; 76:3532–3536. [PubMed: 386341]

Cuello AC, Del Fiacco M, Paxinos G, Somogyi P, Priestley JV. Neuropeptides in striatonigral pathways. J Neural Transm. 1981; 51:83–96. [PubMed: 6167672]

Czubayko U, Plenz D. Fast synaptic transmission between striatal spiny projection neurons. Proc Natl Acad Sci U S A. 2002; 99:15764–15769. [PubMed: 12438690]

Day M, Wokosin D, Plotkin JL, Tian X, Surmeier DJ. Differential excitability and modulation of striatal medium spiny neuron dendrites. J Neurosci. 2008; 28:11603–11614. [PubMed: 18987196]

De Vries TJ, Schoffelmeer AN, Delay-Goyet P, Roques BP, Mulder AH. Selective effects of [D-Ser2(O-t-butyl),-Leu5]enkephalyl-Thr6 and [D-Ser2(O-t-butyl),Leu5]enke-phalyl-Thr6 (O-t-butyl), two new enkephalin analogues, on neurotransmitter release and adenylate cyclase in rat brain slices. Eur J Pharmacol. 1989; 170:137–143. [PubMed: 2575993]

DeBoer P, Westerink BH. GABAergic modulation of striatal cholinergic interneurons: an in vivo microdialysis study. J Neurochem. 1994; 62:70–75. [PubMed: 8263546]

Del Fiacco M, Paxinos G, Cuello AC. Neostriatal en-kephalin-immunoreactive neurones project to the globus pallidus. Brain Res. 1982; 231:1–17. [PubMed: 6275943]

DiFiglia M. Synaptic organization of cholinergic neurons in the monkey neostriatum. J Comp Neurol. 1987; 255:245–258. [PubMed: 3819015]

DiFiglia M, Carey J. Large neurons in the primate neostriatum examined with the combined Golgi-electron microscopic method. J Comp Neurol. 1986; 244:36–52. [PubMed: 3950089]

DiFiglia M, Pasik T, Pasik P. Ultrastructure of Golgi-impregnated and gold-toned spiny and aspiny neurons in the monkey neostriatum. J Neurosci. 1980; 2:303–320. [PubMed: 6121017]

DiFiglia M, Aronin N, Martin JB, Pasik T, Pasik P. Light and electron microscopic localization of immunoreactive Leu-en-kephalin in the monkey basal ganglia. J Neurocytol. 1982; 9:471–492. [PubMed: 6160212]

Dimova R, Vuillet J, Nieoullon A, Kerkerian-Le Goff L. Ultrastructural features of the choline acetyltransferase-containing neurons and relationships with nigral dopaminergic and cortical afferent pathways in the rat striatum. Neuroscience. 1993; 53:1059–1071. [PubMed: 7685068]

Ding J, Guzman JN, Tkatch T, Chen S, Goldberg JA, Ebert PJ, Levitt P, Wilson CJ, Hamm HE, Surmeier DJ. RGS4-dependent attenuation of M4 autoreceptor function in striatal cholinergic interneurons following dopamine depletion. Nat Neurosci. 2006; 9:832–842. [PubMed: 16699510]

Ding JB, Guzman JN, Peterson JD, Goldberg JA, Surmeier DJ. Thalamic gating of corticostriatal signaling by cholinergic interneurons. Neuron. 2010; 67:294–307. [PubMed: 20670836]

Dub L, Smith AD, Bolam JP. Identification of synaptic terminals of thalamic or cortical origin in contact with distinct medium-size spiny neurons in the rat neostriatum. J Comp Neurol. 1988; 267:455–471. [PubMed: 3346370]

Elde R, Hökfelt T, Johansson O, Terenius L. Immunohistochemical studies using antibodies to leucine-enkephalin: initial observations on the nervous system of the rat. Neuroscience. 1976; 1:349–351. [PubMed: 11370520]

English DF, Ibanez-Sandoval O, Stark E, Tecuapetla F, Buzsáki G, Deisseroth K, Tepper JM, Koos T. GABAergic circuits mediate the reinforcement-related signals of striatal cholinergic interneurons. Nat Neurosci. 2012; 15:123–130. [PubMed: 22158514]

Fonnum F, Storm-Mathisen J, Divac I. Biochemical evidence for glutamate as neurotransmitter in corticostriatal and corticothalamic fibres in rat brain. Neuroscience. 1981; 6:863–873. [PubMed: 6113562]

Fujiyama F, Fritschy JM, Stephenson FA, Bolam JP. Synaptic localization of GABA(A) receptor subunits in the striatum of the rat. J Comp Neurol. 2000; 416:158–172. [PubMed: 10581463]

Galvan A, Wichmann T. GABAergic circuits in the basal ganglia and movement disorders. Prog Brain Res. 2007; 160:287–312. [PubMed: 17499121]

Garber, JC.; Barbee, RW.; Bielitzki, JT.; Clayton, LA.; Donovan, JC.; Hendriksen, CFM.; Kohn, DF.; Lipman, NS.; Locke, PA.; Melcher, J.; Quimby, FW.; Turner, PV.; Wood, GA.; Würbel, H. Guide for the care and use of laboratory animals. Washington, DC: The National Academies Press; 2010.

Gerfen CR. Synaptic organization of the striatum. J Electron Microsc Tech. 1988; 10:265–281. [PubMed: 3069970]

Gerfen CR, Surmeier DJ. Modulation of striatal projection systems by dopamine. Annu Rev Neurosci. 2011; 34:441–66. [PubMed: 21469956]

Gerfen CR, Engber TM, Mahan LC, Susel Z, Chase TN, Monsma FJ Jr, Sibley DR. D1 and D2 dopamine receptor-regulated gene expression of striatonigral and striatopallidal neurons. Science. 1990; 250:1429–1432. [PubMed: 2147780]

Gerfen CR, McGinty JF, Young WS 3rd. Dopamine differentially regulates dynorphin, substance P, and enkephalin expression in striatal neurons: in situ hybridization histochemical analysis. J Neurosci. 1991; 11:1016–1031. [PubMed: 1707092]

German DC, Bruce G, Hersh LB. Immunohistochemical staining of cholinergic neurons in the human brain using a polyclonal antibody to human choline acetyltransferase. Neurosci Lett. 1985; 61:1–5. [PubMed: 3908999]

Goldberg JA, Ding JB, Surmeier DJ. Muscarinic modulation of striatal function and circuitry. Handb Exp Pharmacol. 2012; 208:223–241. [PubMed: 22222701]

Gonzales KK, Pare JF, Jenkins S, Wichmann T, Smith Y. Intrinsic microcircuitry of GABAergic inputs from direct and indirect striatofugal neurons on striatal cholinergic interneurons in the primate putamen. Soc Neurosci Abstr. 2009; 828:4.

Gonzales KK, Pare JF, Jenkins S, Wichmann T, Smith Y. Striatal cholinergic interneurons receive intrinsic GABAergic inputs from axon collaterals of direct and indirect striatofugal neurons in the primate putamen. IBAGS X Abstr. 2010:61.

Gonzales KK, Pare JF, Wichmann T, Smith Y. GABAergic microcircuitry of cholinergic interneurons in the monkey putamen. Soc Neurosci Abstr. 2011; 245:02.

Govindaiah G, Wang Y, Cox CL. Substance P selectively modulates GABA(A) receptor-mediated synaptic transmission in striatal cholinergic interneurons. Neuropharmacology. 2010; 58:413–422. [PubMed: 19786036]

Graveland GA, DiFiglia M. The frequency and distribution of medium-sized neurons with indented nuclei in the primate and rodent neostriatum. Brain Res. 1985; 327:307–311. [PubMed: 3986508]

Graybiel AM. Neurotransmitters and neuromodulators in the basal ganglia. Trends Neurosci. 1990; 13:244–254. [PubMed: 1695398]

Graybiel AM, Baughman RW, Eckenstein F. Cholinergic neuropil of the striatum observes striosomal boundaries. Nature. 1986; 323:625–627. [PubMed: 3773990]

Haber S, Elde R. Correlation between Met-enkephalin and substance P immunoreactivity in the primate globus pallidus. Neuroscience. 1981; 6:1291–1297. [PubMed: 6167897]

Haber SN. Neurotransmitters in the human and nonhuman primate basal ganglia. Hum Neurobiol. 1986; 5:159–168. [PubMed: 2876974]

Hodgson AJ, Penke B, Erdei A, Chubb IW, Somogyi P. Antisera to gamma-aminobutyric acid. I. Production and characterization using a new model system. J Histochem Cytochem. 1985; 33:229–239. [PubMed: 3973378]

Holt DJ, Graybiel AM, Saper CB. Neurochemical architecture of the human striatum. J Comp Neurol. 1997; 384:1–25. [PubMed: 9214537]

Holt DJ, Herman MM, Hyde TM, Kleinman JE, Sinton CM, German DC, Hersh LB, Graybiel AM, Saper CB. Evidence for a deficit in cholinergic interneurons in the striatum in schizophrenia. Neuroscience. 1999; 94:21–31. [PubMed: 10613493]

Hutcherson L, Roberts RC. The immunocytochemical localization of substance P in the human striatum: a postmortem ultrastructural study. Synapse. 2005; 57:191–201. [PubMed: 15986364]

Ingham CA, Hood SH, Arbuthnott GW. A light and electron microscopical study of enkephalin-immunoreactive structures in the rat neostriatum after removal of the nigrostriatal dopaminergic pathway. Neuroscience. 1991; 42:715–730. [PubMed: 1683475]

Izquierdo I. Acetylcholine release is modulated by different opioid receptor types in different brain regions and species. Trends Pharmacol Sci. 1990; 11:179–180. [PubMed: 2160747]

Izzo PN, Bolam JP. Cholinergic synaptic input to different parts of spiny striatonigral neurons in the rat. J Comp Neurol. 1988; 269:219–234. [PubMed: 3281983]

Jabourian M, Bourgoin S, Perez S, Godeheu G, Glowinski J, Kemel ML. Mu opioid control of the N-methyl-D-aspartate-evoked release of [^{3}H]-acetylcholine in the limbic territory of the rat striatum in vitro: diurnal variations and implication of a dopamine link. Neuroscience. 2004; 123:733–742. [PubMed: 14706785]

Jabourian M, Venance L, Bourgoin S, Ozon S, Perez S, Godeheu G, Glowinski J, Kemel ML. Functional mu opioid receptors are expressed in cholinergic interneurons of the rat dorsal striatum: territorial specificity and diurnal variation. Eur J Neurosci. 2005; 21:3301–3309. [PubMed: 16026468]

Jaeger D, Kita H, Wilson CJ. Surround inhibition among projection neurons is weak or nonexistent in the rat neostriatum. J Neurophysiol. 1994; 72:2555–2558. [PubMed: 7884483]

Jiang ZG, North RA. Pre- and postsynaptic inhibition by opioids in rat striatum. J Neurosci. 1992; 12:356–361. [PubMed: 1309576]

Joshua M, Adler A, Mitelman R, Vaadia E, Bergman H. Midbrain dopaminergic neurons and striatal cholinergic interneurons encode the difference between reward and aversive events at different epochs of probabilistic classical conditioning trials. J Neurosci. 2008; 28:11673–11684. [PubMed: 18987203]

Joyce JN. Differential response of striatal dopamine and muscarinic cholinergic receptor subtypes to the loss of dopamine. I. Effects of intranigral or intracerebroventricular 6-hydroxydopamine lesions of the mesostriatal dopamine system. Exp Neurol. 1991; 113:261–76. [PubMed: 1833219]

Joyce JN. Differential response of striatal dopamine and muscarinic cholinergic receptor subtypes to the loss of dopamine. III. Results in Parkinson's disease cases. Brain Res. 1993; 600:156–160. [PubMed: 8422582]

Kaneko T, Shigemoto R, Nakanishi S, Mizuno N. Substance P receptor-immunoreactive neurons in the rat neostriatum are segregated into somatostatinergic and cholinergic aspiny neurons. Brain Res. 1993; 631:297–303. [PubMed: 7907524]

Karson CN, Casanova MF, Kleinman JE, Griffin WS. Choline acetyltransferase in schizophrenia. Am J Psychiatry. 1993; 150:454–459. [PubMed: 8434662]

Kawaguchi Y, Wilson CJ, Augood SJ, Emson PC. Striatal interneurones: chemical, physiological and morphological characterization. Trends Neurosci. 1995; 18:527–535. [PubMed: 8638293]

Kawaguchi Y, Aosaki T, Kubota Y. Cholinergic and GABAergic interneurons in the striatum. Nihon Shinkei Seishin Yakurigaku Zasshi. 1997; 17:87–90. [PubMed: 9201728]

Kemp JM, Powell TP. The synaptic organization of the caudate nucleus. Philos Trans R Soc Lond B Biol Sci. 1971; 262:403–412. [PubMed: 4399121]

Kerr JN, Plenz D. Dendritic calcium encodes striatal neuron output during up-states. J Neurosci. 2002; 22:1499–1512. [PubMed: 11880480]

Kerr JN, Plenz D. Action potential timing determines dendritic calcium during striatal up-states. J Neurosci. 2004; 24:877–885. [PubMed: 14749432]

Kimura M, Rajkowski J, Evarts E. Tonically discharging putamen neurons exhibit set-dependent responses. Proc Natl Acad Sci U S A. 1984; 81:4998–5001. [PubMed: 6589643]

Kita H, Kitai ST. Intracellular study of rat globus pallidus neurons: membrane properties and responses to neostriatal, subthalamic and nigral stimulation. Brain Res. 1991; 564:296–305. [PubMed: 1810628]

Kita H, Tokuno H, Nambu A. Monkey globus pallidus external segment neurons projecting to the neostriatum. Neuroreport. 1999; 10:1467–1472. [PubMed: 10380964]

Kosaka T, Tauchi M, Dahl JL. Cholinergic neurons containing GABA-like and/or glutamic acid decarboxylase-like immunoreactivities in various brain regions of the rat. Exp Brain Res. 1988; 70:605–617. [PubMed: 3384059]

Kubota Y, Kawaguchi Y. Spatial distributions of chemically identified intrinsic neurons in relation to patch and matrix compartments of rat neostriatum. J Comp Neurol. 1993; 332:499–513. [PubMed: 8349845]

Kubota Y, Kawaguchi Y. Dependence of GABAergic synaptic areas on the interneuron type and target size. J Neurosci. 2000; 20:375–386. [PubMed: 10627614]

Kubota Y, Inagaki S, Shimada S, Kito S, Eckenstein F, Tohyama M. Neostriatal cholinergic neurons receive direct synaptic inputs from dopaminergic axons. Brain Res. 1987; 413:179–184. [PubMed: 2885073]

Kubota Y, Mikawa S, Kawaguchi Y. Neostriatal GABAergic interneurones contain NOS, calretinin or parvalbumin. Neuroreport. 1993; 5:205–208. [PubMed: 7507722]

Kuramoto E, Fujiyama F, Unzai T, Nakamura K, Hioki H, Furuta T, Shigemoto R, Ferraguti F, Kaneko T. Metabotropic glutamate receptor 4-immunopositive terminals of medium-sized spiny neurons selectively form synapses with cholinergic interneurons in the rat neostriatum. J Comp Neurol. 2007; 500:908–922. [PubMed: 17177262]

Lapchak PA, Araujo DM, Collier B. Regulation of endogenous acetylcholine release from mammalian brain slices by opiate receptors: hippocampus, striatum and cerebral cortex of guinea-pig and rat. Neuroscience. 1989; 31:313–325. [PubMed: 2552347]

Lapper SR, Bolam JP. Input from the frontal cortex and the parafascicular nucleus to cholinergic interneurons in the dorsal striatum of the rat. Neuroscience. 1992; 51:533–545. [PubMed: 1488113]

Le Moine C, Kieffer B, Gaveriaux-Ruff C, Befort K, Bloch B. Delta-opioid receptor gene expression in the mouse forebrain: localization in cholinergic neurons of the striatum. Neuroscience. 1994; 62:635–640. [PubMed: 7870294]

Lendvai B, Sandor NT, Sandor A. Influence of selective opiate antagonists on striatal acetylcholine and dopamine release. Acta Physiol Hung. 1993; 81:19–28. [PubMed: 8178651]

Lindefors N, Brodin E, Theodorsson-Norheim E, Ungerstedt U. Regional distribution and in vivo release of tachykinin-like immunoreactivities in rat brain: evidence for regional differences in relative proportions of tachykinins. Regul Pept. 1985; 10:217–230. [PubMed: 2581287]

Lindefors N, Brodin E, Tossman U, Segovia J, Ungerstedt U. Tissue levels and in vivo release of tachykinins and GABA in striatum and substantia nigra of rat brain after unilateral striatal dopamine denervation. Exp Brain Res. 1989; 74:527–534. [PubMed: 2468514]

Llorens-Cortes C, Van Amsterdam JG, Giros B, Quach TT, Schwartz JC. Enkephalin biosynthesis and release in mouse striatum are inhibited by GABA receptor stimulation: compared changes in preproenkephalin mRNA and Tyr-Gly-Gly levels. Brain Res Mol Brain Res. 1990; 8:227–233. [PubMed: 2170800]

MacKenzie ML, Stachowiak MK, Zigmond MJ. Dopaminergic inhibition of striatal acetylcholine release after 6-hydroxydopamine. Eur J Pharmacol. 1989; 168:43–52. [PubMed: 2511032]

Mai JK, Stephens PH, Hopf A, Cuello AC. Substance P in the human brain. Neuroscience. 1986; 17:709–739. [PubMed: 2422595]

Mallet N, Micklem BR, Henny P, Brown MT, Williams C, Bolam JP, Nakamura KC, Magill PJ. Dichotomous organization of the external globus pallidus. Neuron. 2012; 74:1075–1086. [PubMed: 22726837]

Martone ME, Armstrong DM, Young SJ, Groves PM. Ultrastructural examination of enkephalin and substance P input to cholinergic neurons within the rat neostriatum. Brain Res. 1992; 594:253–262. [PubMed: 1280527]

Matsumoto N, Minamimoto T, Graybiel AM, Kimura M. Neurons in the thalamic CM-Pf complex supply striatal neurons with information about behaviorally significant sensory events. J Neurophysiol. 2001; 85:960–976. [PubMed: 11160526]

Meredith GE, Wouterlood FG. Hippocampal and midline thalamic fibers and terminals in relation to the choline acetyltransferase-immunoreactive neurons in nucleus accumbens of the rat: a light and electron microscopic study. J Comp Neurol. 1990; 296:204–221. [PubMed: 2358532]

Merighi A, Salio C, Ferrini F, Lossi L. Neuromodulatory function of neuropeptides in the normal CNS. J Chem Neuroanat. 2011; 42:276–287. [PubMed: 21385606]

Miura M, Saino-Saito S, Masuda M, Kobayashi K, Aosaki T. Compartment-specific modulation of GABAergic synaptic transmission by mu-opioid receptor in the mouse striatum with green fluorescent protein-expressing dopamine islands. J Neurosci. 2007; 27:9721–9728. [PubMed: 17804632]

Miura M, Masuda M, Aosaki T. Roles of micro-opioid receptors in GABAergic synaptic transmission in the striosome and matrix compartments of the striatum. Mol Neurobiol. 2008; 37:104–115. [PubMed: 18473190]

Morris G, Arkadir D, Nevet A, Vaadia E, Bergman H. Coincident but distinct messages of midbrain dopamine and striatal tonically active neurons. Neuron. 2004; 43:133–143. [PubMed: 15233923]

Mulder AH, Wardeh G, Hogenboom F, Frankhuyzen AL. Kappa- and delta-opioid receptor agonists differentially inhibit striatal dopamine and acetylcholine release. Nature. 1984; 308:278–280. [PubMed: 6322011]

Nanda B, Galvan A, Smith Y, Wichmann T. Effects of stimulation of the centromedian nucleus of the thalamus on the activity of striatal cells in awake rhesus monkeys. Eur J Neurosci. 2009; 29:588–598. [PubMed: 19175404]

Oertel WH, Riethmüller G, Mugnaini E, Schmechel DE, Weindl A, Gramsch C, Herz A. Opioid peptide-like immunoreactivity localized in GABAergic neurons of rat neostriatum and central amygdaloid nucleus. Life Sci. 1983; 33(suppl 1):73–76. [PubMed: 6664248]

Oertel WH, Nitsch C, Mugnaini E. Immunocytochemical demonstration of the GABAergic neurons in rat globus pallidus and nucleus entopeduncularis and their GABAergic innervation. Adv Neurol. 1984; 40:91–98. [PubMed: 6320608]

Parent A, Hazrati LN. Functional anatomy of the basal ganglia. I. The cortico-basal ganglia-thalamo-cortical loop. Brain Res Brain Res Rev. 1995; 20:91–127. [PubMed: 7711769]

Parent A, Cicchetti F, Beach TG. Striatal neurones displaying substance P (NK1) receptor immunoreactivity in human and non-human primates. Neuroreport. 1995; 6:721–724. [PubMed: 7605934]

Pasik P, Pasik T, DiFiglia M. Quantitative aspects of neuronal organization in the neostriatum of the macaque monkey. Res Publ Assoc Res Nerv Ment Dis. 1976; 55:57–90. [PubMed: 827000]

Pasik P, Pasik T, Holstein GR, Hamori J. GABAergic elements in the neuronal circuits of the monkey neostriatum: a light and electron microscopic immunocytochemical study. J Comp Neurol. 1988; 270:157–170. [PubMed: 3379156]

Pasquini F, Bochet P, Garbay-Jaureguiberry C, Roques BP, Rossier J, Beaudet A. Electron microscopic localization of photoaffinity-labelled delta opioid receptors in the neostriatum of the rat. J Comp Neurol. 1992; 326:229–244. [PubMed: 1336020]

Penny GR, Afsharpour S, Kitai ST. The glutamate decarboxylase-, leucine enkephalin-, methionine enkephalin- and substance P-immunoreactive neurons in the neostriatum of the rat and cat: evidence for partial population overlap. Neuroscience. 1986; 17:1011–1045. [PubMed: 2423919]

Perez S, Tierney A, Deniau JM, Kemel ML. Tachykinin regulation of cholinergic transmission in the limbic/pre-frontal territory of the rat dorsal striatum: implication of new neurokinine 1-sensitive receptor binding site and interaction with enkephalin/mu opioid receptor transmission. J Neurochem. 2007; 103:2153–2163. [PubMed: 17949415]

Peters A, Palay SL. The morphology of synapses. J Neurocytol. 1996; 25:687–700. [PubMed: 9023718]

Peters, A.; Palay, SL.; Webster, H., editors. The fine structure of the nervous system: neurons and their supporting cells. 3rd. New York: Oxford University Press; 1991.

Peterson GM, Lanford GW, Powell EW. Fate of septohippocampal neurons following fimbria-fornix transection: a time course analysis. Brain Res Bull. 1990; 25:129–137. [PubMed: 2207699]

Phelps PE, Houser CR, Vaughn JE. Immunocytochemical localization of choline acetyltransferase within the rat neostriatum: a correlated light and electron microscopic study of cholinergic neurons and synapses. J Comp Neurol. 1985; 238:286–307. [PubMed: 4044917]

Phend KD, Weinberg RJ, Rustioni A. Techniques to optimize post-embedding single and double staining for amino acid neurotransmitters. J Histochem Cytochem. 1992; 40:1011–1020. [PubMed: 1376741]

Pickel VM, Chan J. Spiny neurons lacking choline acetyltransferase immunoreactivity are major targets of cholinergic and catecholaminergic terminals in rat striatum. J Neurol Res. 1990; 25:263–280.

Pisani A, Bonsi P, Centonze D, Calabresi P, Bernardi G. Activation of D2-like dopamine receptors reduces synaptic inputs to striatal cholinergic interneurons. J Neurosci. 2000; 20:RC69. [PubMed: 10729358]

Pisani A, Bonsi P, Picconi B, Tolu M, Giacomini P, Scarnati E. Role of tonically-active neurons in the control of striatal function: cellular mechanisms and behavioral correlates. Prog Neuropsychopharmacol Biol Psychiatry. 2001; 25:211–230. [PubMed: 11263753]

Pisani A, Bernardi G, Ding J, Surmeier DJ. Re-emergence of striatal cholinergic interneurons in movement disorders. Trends Neurosci. 2007; 30:545–553. [PubMed: 17904652]

Plenz D. When inhibition goes incognito: feedback interaction between spiny projection neurons in striatal function. Trends Neurosci. 2003; 26:436–443. [PubMed: 12900175]

Rasband, WS. Image J. Bethesda, MD: U. S. National Institutes of Health; 1997–2012.

Ravel S, Legallet E, Apicella P. Responses of tonically active neurons in the monkey striatum discriminate between motivationally opposing stimuli. J Neurosci. 2003; 23:8489–8497. [PubMed: 13679417]

Raz A, Feingold A, Zelanskaya V, Vaadia E, Bergman H. Neuronal synchronization of tonically active neurons in the striatum of normal and parkinsonian primates. J Neurophysiol. 1996; 763:2083–2088. [PubMed: 8890317]

Raz A, Frechter-Mazar V, Feingold A, Abeles M, Vaadia E, Bergman H. Activity of pallidal and striatal tonically active neurons is correlated in mptp-treated monkeys but not in normal monkeys. J Neurosci. 2001; 21:RC128. [PubMed: 11157099]

Reiner A, Medina L, Haber SN. The distribution of dynorphinergic terminals in striatal target regions in comparison to the distribution of substance P-containing and enkephalinergic terminals in monkeys and humans. Neuroscience. 1999; 88:775–793. [PubMed: 10363817]

Reynolds JN, Wickens JR. The corticostriatal input to giant aspiny interneurons in the rat: a candidate pathway for synchronising the response to reward-related cues. Brain Res. 2004; 1011:115–128. [PubMed: 15140651]

Ribak CE, Roberts RC. GABAergic synapses in the brain identified with antisera to GABA and its synthesizing enzyme, glutamate decarboxylase. J Electron Microsc Tech. 1990; 15:34–48. [PubMed: 2187069]

Richardson PJ, Dixon AK, Lee K, Bell MI, Cox PJ, Williams R, Pinnock RD, Freeman TC. Correlating physiology with gene expression in striatal cholinergic neurones. J Neurochem. 2000; 74:839–846. [PubMed: 10646537]

Roberts RC, Gaither LA, Peretti FJ, Lapidus B, Chute DJ. Synaptic organization of the human striatum: a postmortem ultrastructural study. J Comp Neurol. 1996; 374:523–534. [PubMed: 8910733]

Ruzicka BB, Day R, Jhamandas K. Quinolinic acid elevates striatal and pallidal Met-enkephalin levels: the role of enkephalin synthesis and release. Brain Res. 1991; 562:117–125. [PubMed: 1839239]

Sadikot AF, Parent A, Smith Y, Bolam JP. Efferent connections of the centromedian and parafascicular thalamic nuclei in the squirrel monkey: a light and electron microscopic study of the thalamostriatal projection in relation to striatal heterogeneity. J Comp Neurol. 1992a; 315:228–242. [PubMed: 1619051]

Sadikot AF, Parent A, Francois C. Efferent connections of the centromedian and parafascicular thalamic nuclei in the squirrel monkey: a PHA-L study of subcortical projections. J Comp Neurol. 1992b; 315:137–159. [PubMed: 1372010]

Sato F, LavalÍe P, Ĺvesque M, Parent A. Single-axon tracing study of neurons of the external segment of the globus pallidus in primate. J Comp Neurol. 2000; 417:17–31. [PubMed: 10660885]

Semba K, Fibiger HC, Vincent SR. Neurotransmitters in the mammalian striatum: neuronal circuits and heterogeneity. Can J Neurol Sci. 1987; 14(3 suppl):386–394. [PubMed: 2445456]

Shiromani PJ, Armstrong DM, Bruce G, Hersh LB, Groves PM, Gillin JC. Relation of pontine choline acetyltransferase immunoreactive neurons with cells which increase discharge during REM sleep. Brain Res Bull. 1987; 18:447–455. [PubMed: 3580914]

Shiromani PJ, Lai YY, Siegel JM. Descending projections from the dorsolateral pontine tegmentum to the paramedian reticular nucleus of the caudal medulla in the cat. Brain Res. 1990; 517:224–228. [PubMed: 1695862]

Sidibe M, Smith Y. Thalamic inputs to striatal interneurons in monkeys: synaptic organization and co-localization of calcium binding proteins. Neuroscience. 1999; 89:1189–1208. [PubMed: 10362307]

Sizemore RJ, Reynolds JN, Oorschot DE. Number and type of synapses on the distal dendrite of a rat striatal cholinergic interneuron: a quantitative, ultrastructural study. J Anat. 2010; 217:223–235. [PubMed: 20629984]

Smith ML, Deadwyler SA, Booze RM. 3-D reconstruction of the cholinergic basal forebrain system in young and aged rats. Neurobiol Aging. 1993; 14:389–392. [PubMed: 8367020]

Smith ML, Hale BD, Booze RM. Calbindin-D28k immunoreactivity within the cholinergic and GABAergic projection neurons of the basal forebrain. Exp Neurol. 1994; 130:230–236. [PubMed: 7867752]

Smith Y, Parent A, Seguela P, Descarries L. Distribution of GABA-immunoreactive neurons in the basal ganglia of the squirrel monkey (*Saimiri sciureus*). J Comp Neurol. 1987; 259:50–64. [PubMed: 3294929]

Smith Y, Bennett BD, Bolam JP, Parent A, Sadikot AF. Synaptic relationships between dopaminergic afferents and cortical or thalamic input in the sensorimotor territory of the striatum in monkey. J Comp Neurol. 1994; 344:1–19. [PubMed: 7914894]

Smith Y, Bevan MD, Shink E, Bolam JP. Microcircuitry of the direct and indirect pathways of the basal ganglia. Neuroscience. 1998; 86:353–387. [PubMed: 9881853]

Smith Y, Raju DV, Pare JF, Sidibe M. The thalamostriatal system: a highly specific network of the basal ganglia circuitry. Trends Neurosci. 2004; 27:520–527. [PubMed: 15331233]

Smith Y, Raju D, Nanda B, Pare JF, Galvan A, Wichmann T. The thalamostriatal systems: anatomical and functional organization in normal and parkinsonian states. Brain Res Bull. 2009; 78:60–68. [PubMed: 18805468]

Somogyi P, Hodgson AJ. Antisera to gamma-aminobutyric acid. III. Demonstration of GABA in Golgi-impregnated neurons and in conventional electron microscopic sections of cat striate cortex. J Histochem Cytochem. 1985; 33:249–257. [PubMed: 2579124]

Stern EA, Jaeger D, Wilson CJ. Membrane potential synchrony of simultaneously recorded striatal spiny neurons in vivo. Nature. 1998; 394:475–478. [PubMed: 9697769]

Sullivan MA, Chen H, Morikawa H. Recurrent inhibitory network among striatal cholinergic interneurons. J Neurosci. 2008; 28:8682–8690. [PubMed: 18753369]

Surmeier DJ. The role of dopamine in modulating the structure and function of striatal circuits. Prog Brain Res. 2010; 183:149–167. [PubMed: 20696319]

Surmeier DJ, Kita H, Kitai ST. The expression of gamma-aminobutyric acid and Leu-enkephalin immunoreactivity in primary monolayer cultures of rat striatum. Brain Res. 1988; 470:265–282. [PubMed: 3064876]

Suzuki T, Miura M, Nishimura K, Aosaki T. Dopamine-dependent synaptic plasticity in the striatal cholinergic interneurons. J Neurosci. 2001; 21:6492–6501. [PubMed: 11517238]

Taniyama K, Nitsch C, Wagner A, Hassler R. Aspartate, glutamate and GABA levels in pallidum, substantia nigra, center median and dorsal raphe nuclei after cylindric lesion of caudate nucleus in cat. Neurosci Lett. 1980; 16:155–160. [PubMed: 6133240]

Taverna S, Ilijic E, Surmeier DJ. Recurrent collateral connections of striatal medium spiny neurons are disrupted in models of Parkinson's disease. J Neurosci. 2008; 28:5504–5512. [PubMed: 18495884]

Tecuapetla F, Carrillo-Reid L, Guzmán JN, Galarraga E, Bargas J. Different inhibitory inputs onto neostriatal projection neurons as revealed by field stimulation. J Neurophysiol. 2005; 93:1119–1126. [PubMed: 15356181]

Tepper JM, Bolam JP. Functional diversity and specificity of neostriatal interneurons. Curr Opin Neurobiol. 2004; 14:685–692. [PubMed: 15582369]

Tepper JM, Koos T, Wilson CJ. GABAergic microcircuits in the neostriatum. Trends Neurosci. 2004; 27:662–669. [PubMed: 15474166]

Tepper JM, Wilson CJ, Koos T. Feedforward and feedback inhibition in neostriatal GABAergic spiny neurons. Brain Res Rev. 2008; 58:272–281. [PubMed: 18054796]

Tepper JM, Tecuapetla F, Koós T, Ibanez-Sáñdoval O. Heterogeneity and diversity of striatal GABAergic interneurons. Front Neuroanat. 2010; 4:150. [PubMed: 21228905]

Thomas TM, Smith Y, Levey AI, Hersch SM. Cortical inputs to m2-immunoreactive striatal interneurons in rat and monkey. Synapse. 2000; 37:252–261. [PubMed: 10891862]

Tunstall MJ, Oorschot DE, Kean A, Wickens JR. Inhibitory interactions between spiny projection neurons in the rat striatum. J Neurophysiol. 2002; 88:1263–1269. [PubMed: 12205147]

Vuillet J, Dimova R, Nieoullon A, Kerkerian-Le Goff L. Ultrastructural relationships between choline acetyltransferase- and neuropeptide Y-containing neurons in the rat striatum. Neuroscience. 1992; 46:351–360. [PubMed: 1542411]

Waldvogel HJ, Billinton A, White JH, Emson PC, Faull RL. Comparative cellular distribution of GABAA and GABAB receptors in the human basal ganglia: immunohistochemical colocalization of the alpha 1 subunit of the GABAA receptor, and the GABABR1 and GABABR2 receptor subunits. J Comp Neurol. 2004; 470:339–356. [PubMed: 14961561]

Williams RG, Dockray GJ. Distribution of enkephalin-related peptides in rat brain: immunohistochemical studies using antisera to met-enkephalin and met-enkephalin Arg6-Phe7. Neuroscience. 1983; 9:563–586. [PubMed: 6312371]

Wilson CJ. GABAergic inhibition in the neostriatum. Prog Brain Res. 2007; 160:91–110. [PubMed: 17499110]

Wilson CJ, Groves PM. Fine structure and synaptic connections of the common spiny neuron of the rat neostriatum: a study employing intracellular inject of horseradish peroxidase. J Comp Neurol. 1980; 194:599–615. [PubMed: 7451684]

Wolansky T, Pagliardini S, Greer JJ, Dickson CT. Immunohistochemical characterization of substance P receptor (NK(1)R)-expressing interneurons in the entorhinal cortex. J Comp Neurol. 2007; 502:427–441. [PubMed: 17366610]

Wu Y, Parent A. Striatal interneurons expressing calretinin, parvalbumin or NADPH-diaphorase: a comparative study in the rat, monkey and human. Brain Res. 2000; 863:182–191. [PubMed: 10773206]

Yan Z, Surmeier DJ. D5 dopamine receptors enhance Zn2+-sensitive GABA(A) currents in striatal cholinergic interneurons through a PKA/PP1 cascade. Neuron. 1997; 19:1115–1126. [PubMed: 9390524]

Yelnik J, Francois C, Percheron G, Tande D. Morphological taxonomy of the neurons of the primate striatum. J Comp Neurol. 1991; 313:273–294. [PubMed: 1722488]

Yelnik J, Percheron G, Francois C, Garnier A. Cholinergic neurons of the rat and primate striatum are morphologically different. Prog Brain Res. 1993; 99:25–34. [PubMed: 8108552]

Young AB, Bromberg MB, Penney JB Jr. Decreased glutamate uptake in subcortical areas deafferented by sensorimotor cortical ablation in the cat. J Neurosci. 1981; 1:241–249. [PubMed: 6114994]

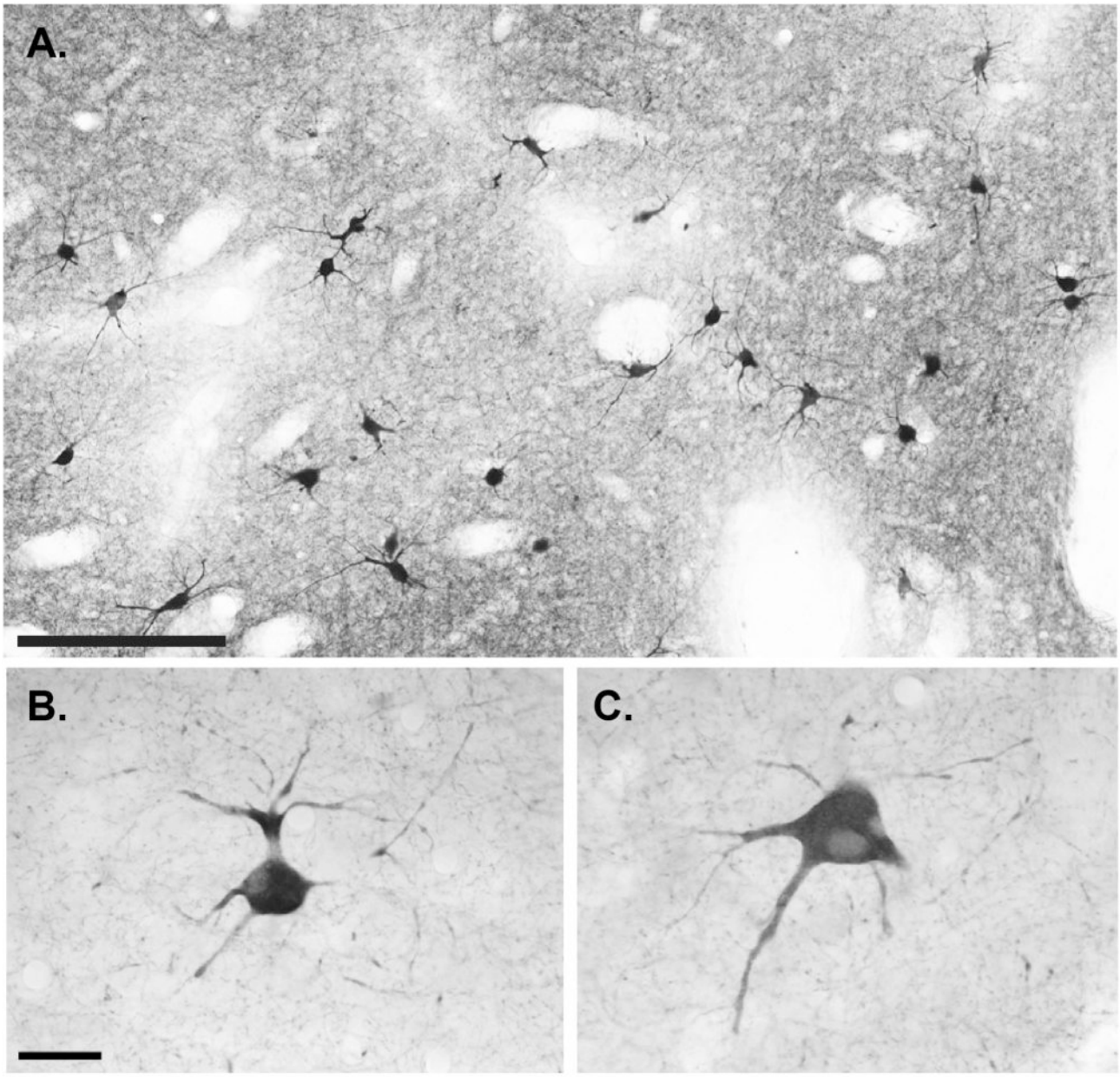

Figure 1.

General pattern of distribution and morphology of cholinergic interneurons in the monkey putamen at the light microscopic level. **A:** Low-power view of ChAT-positive neurons and neuropil in the postcommissural putamen**. B,C:** High-power views of typical ChIs from the monkey sensorimotor putamen. Note that the ChAT-labeled somata have thick primary dendrites from which emerge multiple dendritic branches that extend over long distances in the surrounding neuropil. Scale bar = 100 μm in A; 25 μm in B (applies to B,C).

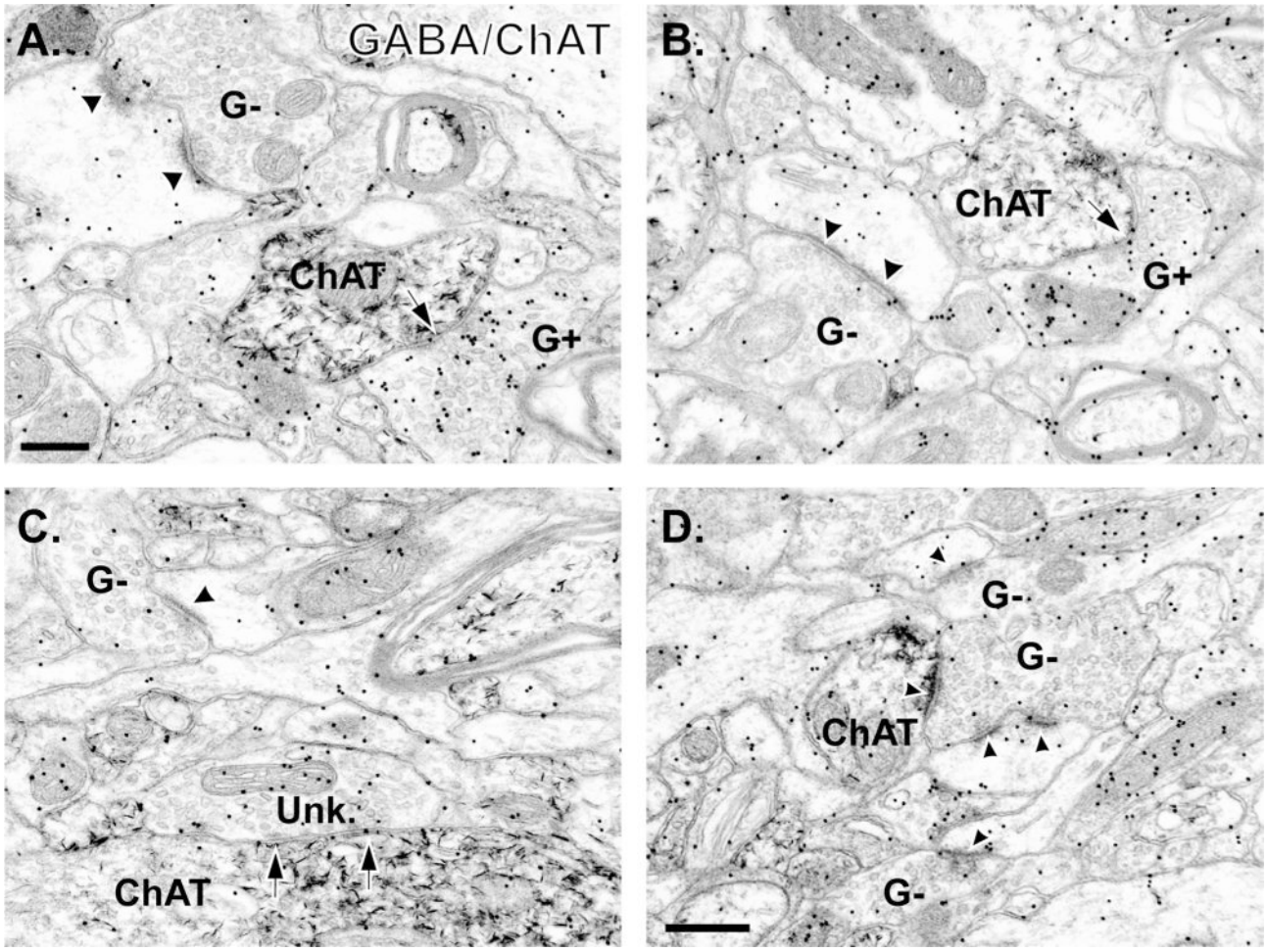

Figure 2.

Electron micrographs of tissue double immunostained for GABA (immunogold) and ChAT (immunoperoxidase) in the monkey putamen. **A,B:** Photomicrographs demonstrating GABA-positive (G+) terminals forming symmetric synapses (arrows) with medium-sized ChAT-labeled dendrites. Note that a GABA-negative (G−) terminal in each micrograph is forming an asymmetric synapse (black arrowheads) with a spine. **C:** Example of a terminal categorized as “symmetric/unknown” (Unk.) that forms a symmetric synapse (black arrows) with a large-sized ChAT-positive dendrite. A GABA-negative (G−) terminal forming an axo-spinous synapse (arrowhead) is also visible. **D:** Example of a GABA-negative terminal forming an asymmetric synapse onto a small-sized ChAT-labeled dendrite and an unlabeled spine (arrowheads). Other GABA-negative (G−) terminals are also visible in this tissue. Scale bar = 0.2 μm in A (applies to A,B); 0.5 μm in D (applies to C,D).

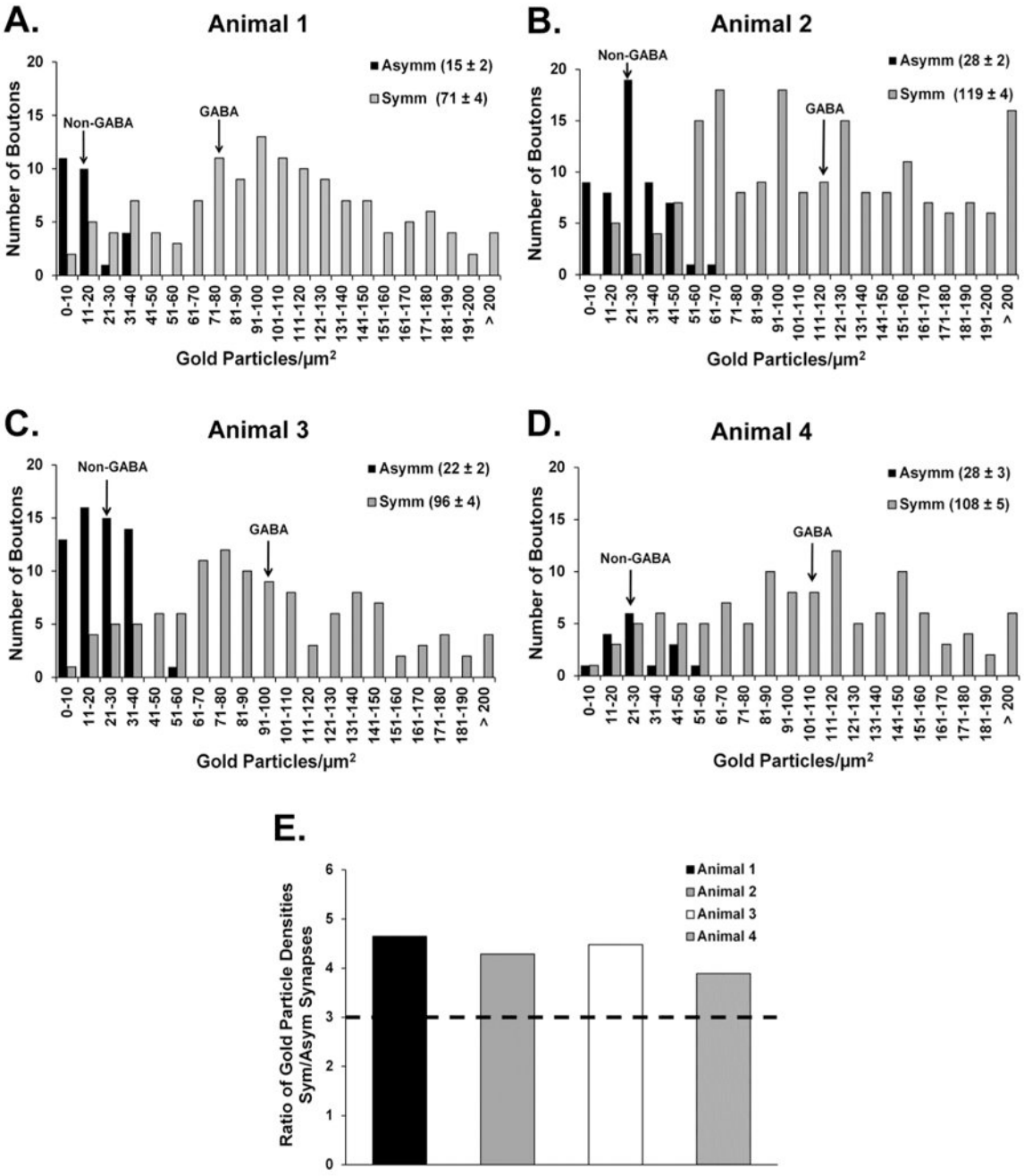

Figure 3.

Frequency distribution histograms of the relative gold particle density in terminals forming synapses with ChAT-labeled elements in the four animals used for the GABA (immunogold) and ChAT (immunoperoxidase) reactions in the monkey putamen. **A–D:** Histograms showing the overall distribution of gold particle densities over terminals forming symmetric (Symm) or asymmetric (Asymm) synapses with ChIs in the postcommissural putamen of each of the animals. The average surface density of gold particles (± SEM) measured in each category of terminals is provided in the legend at the upper right corner of each panel and is indicated by arrows in the histograms pointing to the non-GABA and

GABA means for each animal. The symmetric and asymmetric terminals analyzed in each monkey were collected from blocks of striatal tissue processed from the same double-label immunoreaction. **E:** Comparison of the average ratio of gold particle densities over terminals forming Symm versus Asymm synapses with cholinergic elements in each monkey. A gold particle density ratio of 3 (dashed line in E) between Symm and Asymm terminals served as an (arbitrary) cutoff to separate confirmed GABAergic from “unknown” symmetric terminals.

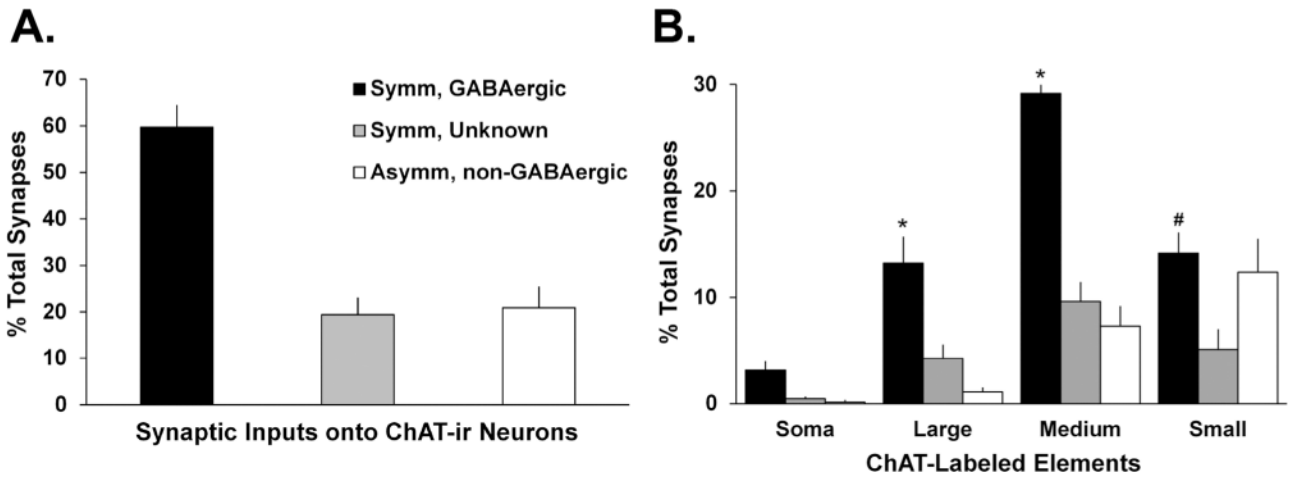

Figure 4.

Proportion of GABAergic and non-GABAergic terminals in contact with ChAT-labeled neurons in the putamen of four monkeys. **A:** Mean percentage (± SEM) of terminals categorized as "symmetric/GABAergic," "symmetric/unknown," or "asymmetric/non-GABAergic." These categories were based on the relative density of gold particle labeling in terminals forming synaptic contact with ChAT-containing neurons. The gold particle density criteria for each terminal category are described in the legend of Figure 3 and in the text. **B:** Comparison of the distribution of the different categories of terminals along the entire somatodendritic domain of striatal cholinergic interneurons. The legend key used in A also applies here. *, $P < 0.001$ Symm, GABAergic versus Symm, Unknown and Asymm, non-GABAergic; #, $P < 0.001$ Symm/GABAergic versus Symm, Unknown.

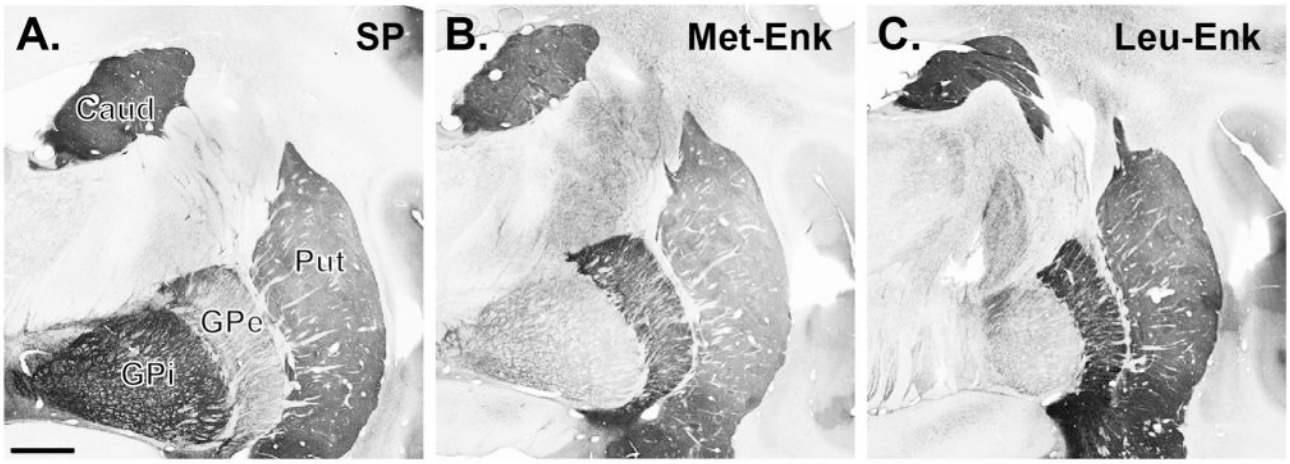

Figure 5.
Light microscopic distribution of the immunoreactivity for SP (**A**), Met-Enk (**B**), and Leu-Enk (**C**) in the monkey striatopallidal complex. SP labeling is intense in the caudate nucleus (CD), putamen (Put), and internal globus pallidus (GPi), whereas strong Met- and Leu-Enk immunostaining is found in the CD, Put, and external globus pallidus (GPe). Scale bar = 2 mm in A (applies to A–C).

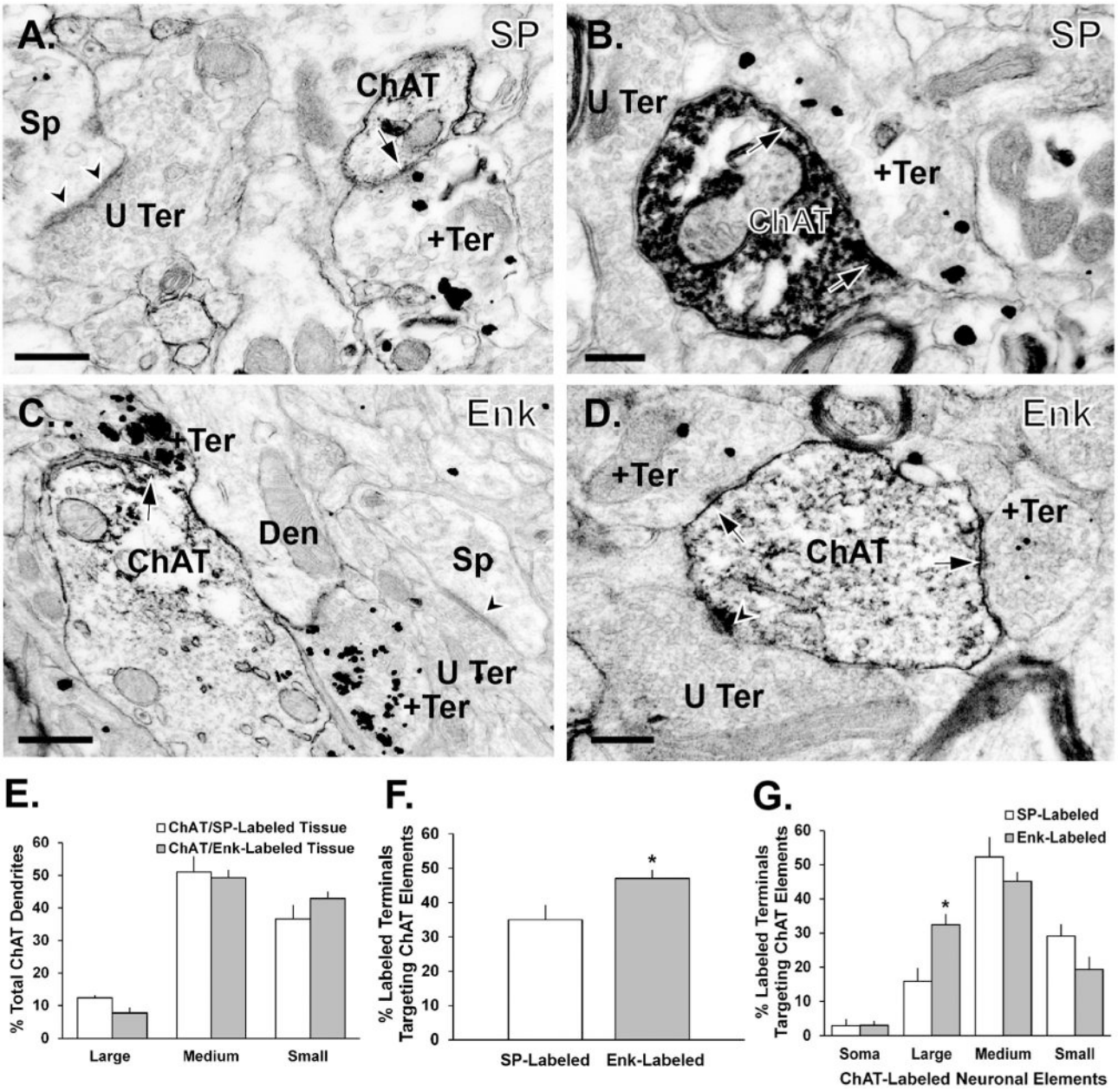

Figure 6.

Synaptic relationships between terminals immunostained for SP or Met-/Leu-Enk (immunogold) and ChAT-immunoreactive dendrites (immunoperoxidase) in the monkey putamen. **A,B:** Photomicrographs showing SP-ir boutons (+Ter) forming symmetric synapses (black arrows) with a small-sized and a medium-sized ChAT-labeled dendrite (A and B, respectively). **C,D:** Examples of Enk-ir terminals (+Ter) forming symmetric synapses (arrows) with a large-sized (C) and a medium-sized (D) ChAT-labeled dendrite. Note examples of unlabeled boutons (U Ter) forming asymmetric synapses (arrowheads) with spines (Sp) in the same fields of view. **E:** Mean percentages (± SEM) of ChAT-ir dendrites of different sizes in the double-immunostained tissue for SP/ChAT (n = 5 animals) or Enk/ChAT (n = 4 animals). **F:** Mean percentages (± SEM) of SP-positive and Enk-positive terminals in contact with ChAT-ir elements in the monkey putamen. *, $P < 0.005$.

G: Mean percentages (± SEM) of SP- and Enk-ir terminals in contact with ChAT-immunoreactive soma and dendrites of various sizes. *, $P = 0.012$ Enk-labeled versus SP-labeled on large dendrites. Abbreviations: Den, dendrite. Scale bar = 0.5 μm in A,C; 0.2 μm in B,D.

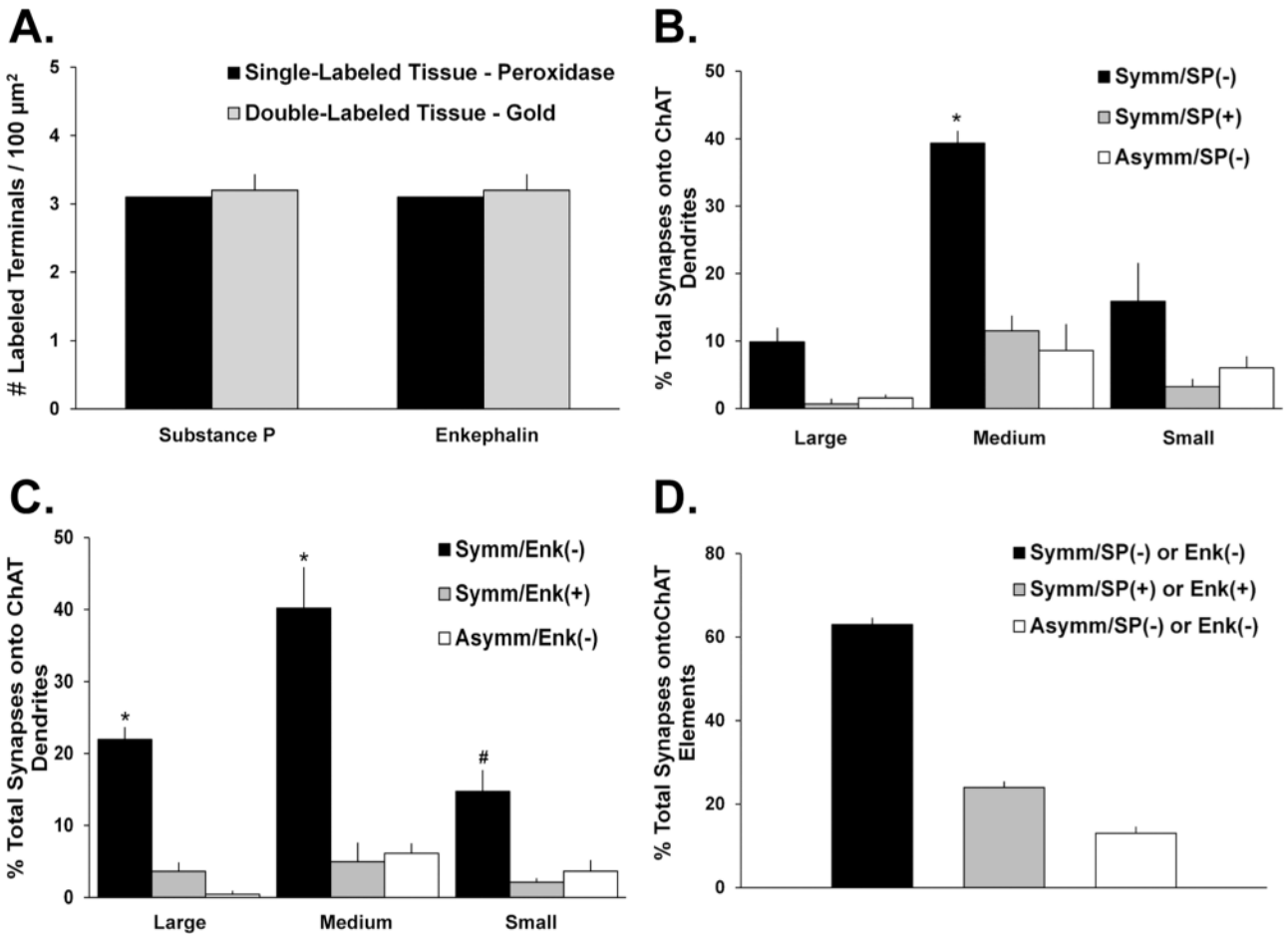

Figure 7.

Proportion of total synaptic inputs onto ChIs from SP- and Enk-ir terminals. **A:** Comparison of the mean densities of SP- or Enk-positive terminals as revealed with the pre-embedding immunogold method in double-immunostained striatal tissue of three monkeys (SP/ChAT-left gray bar; Enk/ChAT-right gray bar) with the density of these terminals in striatal tissue from one monkey single labeled for each peptide with the immunoperoxidase method. The density of labeled terminals for either SP or Enk is the same irrespective of the marker used in single or double immunolabeling reactions. **B,C:** Mean percentages (± SEM) of total terminals in synaptic contact with ChI dendrites in the monkey putamen. Terminals are categorized based on their type of synaptic specializations (symmetric vs. asymmetric) and neuropeptide immunoreactivity (SP+ vs. SP− in B; Enk+ vs. Enk− in C). In B, *, $P < 0.001$ Symm/SP(−) versus Symm/SP(+) and Asymm/SP(−) on medium dendrites. In C, *, $P < 0.001$, Symm/Enk(−) versus Symm/Enk(+) and Asymm/Enk(−) on large or medium dendrites; #, Symm/Enk(−) versus Symm/Enk(+) on small dendrites. **D:** Mean percentages of synaptic inputs onto ChIs that originate from SP+ and Enk+ collaterals of GABAergic striatal projection neurons (Symm/SP+ or Enk+) or other sources of putatively GABAergic terminals (Symm/SP− and Enk−) and putatively glutamatergic boutons (Asymm/SP− and Enk−).

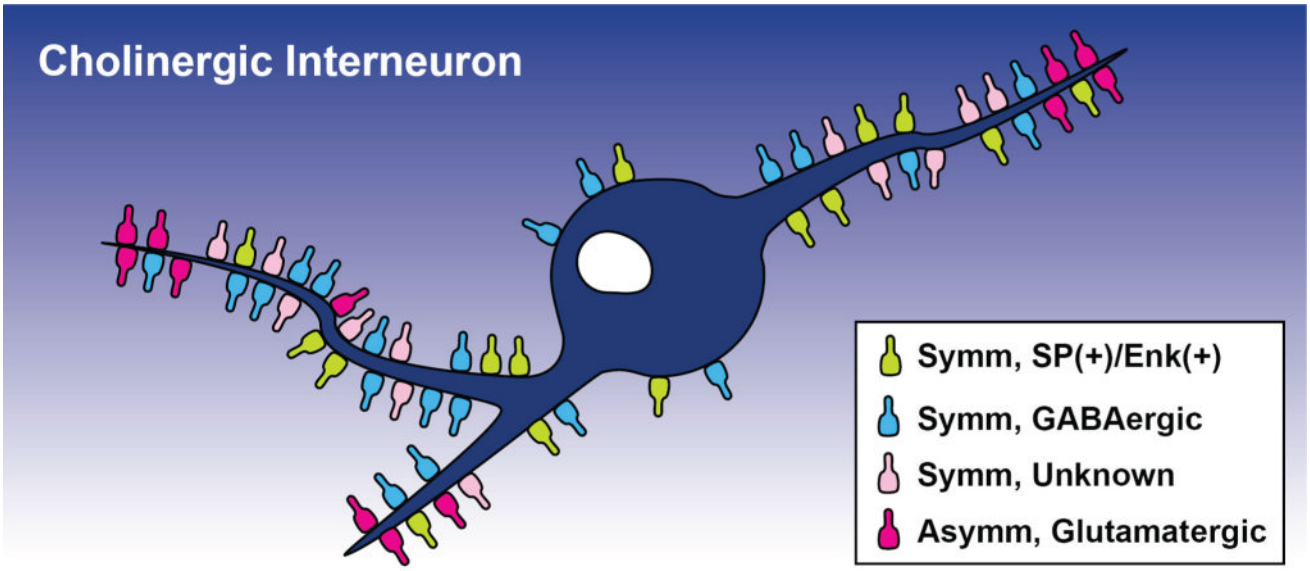

Figure 8.
Schematic of the distribution of various chemically characterized synaptic inputs onto ChIs in the monkey putamen based on results shown in this study. The relative location and proportion of the different terminal subtypes along the somatodendritic domain of ChIs are represented. [Color figure can be viewed in the online issue, which is available at wileyonlinelibrary.com.]

Table 1
Primary Antibodies Used in This Study

Antibody	Immunogen	Manufacturer data	Dilution
Choline acetyltransferase	Purified human placental enzyme	Chemicon (AB143), rabbit polyclonal	1:2,000
Choline acetyltransferase	Purified human placental enzyme	Pro Sci (50–265), goat polyclonal	1:100
Substance P	Synthetic peptide corresponding to the full substance P protein conjugated to BSA	Millipore (MAB356), rat monoclonal	1:200
Methionine-enkephalin	Synthetic Met^5-ENK peptide (H-TGGPM-OH) conjugated through the N-terminal tyrosine to BSA	Millipore (AB5026), rabbit polyclonal	1:1,000
Leucine-enkephalin	Synthetic Leu^5-ENK peptide (H-TGGPL-OH) conjugated through the N-terminal tyrosine to BSA	Millipore (AB5024), rabbit polyclonal	1:1,000
γ-Aminobutyric acid	GABA-BSA	Sigma (A2052), rabbit polyclonal	1:1,000